NACA

RESEARCH MEMORANDUM

TESTS OF AERODYNAMICALLY HEATED MULTIWEB WING

STRUCTURES IN A FREE JET AT MACH NUMBER 2

THREE ALUMINUM-ALLOY MODELS AND ONE STEEL MODEL OF

20-INCH CHORD AND SPAN WITH VARIOUS INTERNAL

STRUCTURES AND SKIN THICKNESSES

By Richard Rosecrans, Louis F. Vosteen,
and William J. Batdorf, Jr.

Langley Aeronautical Laboratory
Langley Field, Va.

NATIONAL ADVISORY COMMITTEE
FOR AERONAUTICS
WASHINGTON

October 28, 1957
Declassified October 31, 1958

NATIONAL ADVISORY COMMITTEE FOR AERONAUTICS

RESEARCH MEMORANDUM

TESTS OF AERODYNAMICALLY HEATED MULTIWEB WING

STRUCTURES IN A FREE JET AT MACH NUMBER 2

THREE ALUMINUM-ALLOY MODELS AND ONE STEEL MODEL OF

20-INCH CHORD AND SPAN WITH VARIOUS INTERNAL

STRUCTURES AND SKIN THICKNESSES

By Richard Rosecrans, Louis F. Vosteen,
and William J. Batdorf, Jr.

SUMMARY

Four multiweb wing structures, representative of airplane or mis-
sile wings, were tested at a Mach number of 2, sea-level static pressure,
an angle of attack of 0°, and a stagnation temperature of approximately
500° F. Three models were of 2024-T3 aluminum alloy and one was of
SAE 1010 steel. Internal structure and skin thickness varied from model
to model. Measurements were made of temperatures, strains, and pressures.
One model failed dynamically under the combined action of aerodynamic
heating and loading. The other models survived, but the steel model
showed small permanent buckles in one skin at the end of the test. Skin
temperatures and pressures are compared with calculated values.

INTRODUCTION

As part of an investigation of the structural effects of aerodynamic
heating, multiweb wing structures have been tested under aerodynamic con-
ditions similar to those encountered in supersonic flight. All tests
have been made at a Mach number of 2 in a free jet and at sea-level static
pressure. The first model, MW-1, was tested to determine temperature dis-
tribution only, but a dynamic failure occurred as a result of the combined
influence of aerodynamic heating and loading. (See ref. 1.)

The unexpected failure of model MW-1 led to subsequent tests to
obtain additional information regarding strains, pressures, and vibration

modes and frequencies, and to investigate various changes in design which
would prevent failure. Preliminary results of tests of six additional
models were reported in reference 2, but detailed test data were not
included. Reference 3 reported the results of tests on the second and
third models, MW-2 and MW-3, in detail. Model MW-2 was essentially a
half-scale version of model MW-1, and also failed dynamically near the
end of the test. Model MW-3, with a thicker skin but otherwise the same
as model MW-2, failed statically in bending at the root section when
tested at 5° angle of attack after surviving four tests at lesser angles
without damage. The present paper includes test data and skin-temperature
analyses for the last four models discussed in reference 2; namely, MW-4,
MW-5, MW-6, and MW-7. Each of the four models was of 20-inch chord and
span and each incorporated some structural change from model MW-2.

Temperature data were taken on all models; in addition, strain gages
were used for vibration studies on all models, but for strain measurements
on one model only. A few pressure measurements were made on one model.

SYMBOLS

c	specific heat, Btu/(lb)(°F)
H	stagnation pressure, lb/sq in. abs
h	heat-transfer coefficient, Btu/(sq ft)(sec)(°F)
N_{Pr}	Prandtl number
T	skin temperature, °F
T_{aw}	adiabatic-wall temperature, °F
T_s	stagnation temperature, °F
T_∞	free-stream temperature, °F
ΔT	difference between skin and web temperatures
t	time, sec
w	density, lb/cu ft
η_r	recovery factor
τ	thickness, ft

TESTS AND MODELS

Test Facility

The tests were made in the preflight jet of the Langley Pilotless Aircraft Research Station at Wallops Island, Va. This facility is a blowdown wind tunnel in which tests are made in a free jet at the exit of a 27- by 27-inch supersonic nozzle. Details of the test facility are given in the appendix of reference 3.

Models

All models (MW-4, MW-5, MW-6, and MW-7) incorporated some structural variation from model MW-2. They were 5-percent-thick symmetrical circular-arc airfoils with 20-inch chord and span and no taper in plan form or thickness. Details of construction are shown in figure 1. All models had solid leading- and trailing-edge sections and solid root bulkheads with doubler plates near the mounting fixture to strengthen the root connection. Each model had six formed spanwise webs spaced at $2\frac{1}{2}$- inch centers. All models were constructed of 2024-T3 aluminum alloy except model MW-7, which was made of SAE 1010 steel.

Exterior finish.- All models were finished to 35 rms microinches and then painted. The left side of models MW-4 and MW-7 (looking upstream) and both sides of models MW-5 and MW-6 were sprayed with a thin coating of zinc chromate primer and striped with black lacquer to form a grid pattern which aided in studying the motion pictures. (See fig. 2.) On the right side of models MW-4 and MW-7, a variety of thermal indicating paints was applied to test their usefulness as a temperature indicating device.

Model MW-4.- Model MW-4 was the same as model MW-2 except that instead of the heavy, solid tip bulkhead of model MW-2, a lighter bulkhead formed of 0.025-inch-thick material was used to permit freer chordwise expansion in the tip region.

Models MW-5 and MW-6.- Models MW-5 and MW-6 had 0.025-inch-thick chordwise ribs at $2\frac{1}{2}$- inch centers in addition to the webs. Except for these ribs, model MW-5 was the same as model MW-2, but model MW-6 also had a thinner skin (0.051-inch thick as compared to 0.064 inch in model MW-2). The ribs were added to provide additional chordwise stiffness and increase the buckling stress in the chordwise direction.

Model MW-7.- Model MW-7 had 0.018-inch-thick webs, 0.043-inch skin, and a 0.250-inch tip bulkhead. The thinner skin and webs were related to those of model MW-2 in inverse proportion to the square roots of the elastic moduli of steel and aluminum, within the limits of available commercial thicknesses. Thus, approximately the same buckling stress was maintained.

Model Instrumentation

Instrumentation for all models is shown in figure 3. The instrumentation consisted of No. 30 gage iron-constantan thermocouples and SR-4 type AB-7 bakelite wire strain gages. For model MW-7 only, 11 orifices for pressure measurements also were provided. Four of these orifices (numbers 1, 4, 5, and 8) were connected to NACA model 46, six-capsule recording manometers by tubing running downward inside the model and out at the base. Two other orifices (numbers 2 and 3) were connected to the same type of recording device in such a way as to measure the difference in pressure between them. Four more orifices (numbers 6, 7, 9, and 11) were connected by short tubes to NACA model 49-NC miniature electrical pressure gages located inside the model. (See ref. 4.) These latter gages were installed to measure rapid fluctuations in pressure. In addition, another NACA miniature pressure gage was so connected to orifices 10 and 11 that it measured the difference in pressure between them. The number of instruments of each type used on each model are summarized in table 1.

Accuracy

Listed in the following table are the estimated probable errors in individual measurements and the corresponding time constants. The time constant, which is considered independent of the probable error, is defined as the time at which the recorded value of a step function input is 63 percent of the input; at three time constants the response amounts to 95 percent of the input. Errors due to thermocouple installation have not been included, but they are believed to be small.

	Probable error	Time constant
Stagnation pressure	±0.7 lb/sq in.	0.03 sec
Stagnation temperature	±3° F	0.12 sec
Model temperature	±3° F	0.03 sec
Model pressures:		
Recording manometers	±0.2 lb/sq in.	0.04 sec
Manometer tubing		0.01 sec
Miniature gages	±0.7 lb/sq in.	0.03 sec

Miniature gages 6, 7, and 9 had flat frequency response to 300 cycles per second, and gages 10 and 11 had flat frequency response to 100 cycles per second.

Vibration Modes and Frequencies

Prior to the wind-tunnel tests, a survey was made of each of the models to find its natural modes and frequencies. An electromagnetic shaker supplied energy to the model, and the signal from a phonograph-type pickup was fed into an oscilloscope to determine resonance and to trace node lines. Frequencies were measured by a Stroboconn frequency indicator. Results are shown in table 2, and indicate that the ribs in models MW-5 and MW-6 increased the model stiffness substantially. This increase is reflected in the higher frequencies for the same modes, except in the cases of first bending and first torsion (modes A and B). It also is reflected in the change in mode shape as in mode C, and in the fact that some of the higher modes involving chordwise bending (modes F to J, for example) which were present in models MW-2 and MW-4 did not appear at all in models MW-5 and MW-6. Model MW-7 did not exhibit some of the higher modes (F, H, I, and J) found in models MW-2 and MW-4, although from the frequencies for the modes it did have, it appeared to be more flexible than model MW-4.

Test Procedure

Each model was mounted vertically in the jet, root downward, at an angle of attack of 0°, with the leading edge 2 inches downstream from the nozzle exit. (See fig. 2.) The parts of the models and their root attachments which were below the tops of the doubler plates were protected from the airstream by a horizontal fence. A knife edge along the upstream edge of the fence was located 1/8-inch above the lower jet boundary.

Running time was measured from the instant air began to flow from the nozzle, and test conditions were assumed to exist whenever the stagnation pressure exceeded 100 lb/sq in. abs. The nozzle static pressure was held as close to atmospheric pressure as possible in order to provide a uniform flow field, free of shock or expansion waves. A little less than 2 seconds was required to establish test conditions. Except for the test on model MW-4, when the jet was shut down because of the failure of the model, test conditions existed for about 9 or 10 seconds. Throughout each test, signals from each instrument were continuously recorded, and motion pictures were taken by seven 16-millimeter cameras located on both sides of the models and overhead. Three of the cameras ran at speeds varying between 610 and 1,160 frames per second; the others ran at speeds of either 24 or 128 frames per second.

Test Conditions

Stagnation pressure.- Stagnation pressure of the airstream was meas-
ured by total-pressure tubes located in the settling chamber between the
heat accumulator and the nozzle. Variation of the stagnation pressure
with time for each test is shown in figure 4. The solid lines represent
values obtained by averaging results from two total-pressure tubes. The
dashed lines represent average values for the period during which test
conditions were assumed to exist (that is, when $H \geqq 100$ lb/sq in. abs).
For the test on model MW-4, values for only the first 6 seconds were con-
sidered for averaging since the model failed between 5 and 6 seconds.

Stagnation temperature.- The stagnation temperature of the airstream
was measured by iron-constantan thermocouples placed in two probes
$1\frac{1}{2}$ inches downstream and 4 inches on each side of the trailing edge of
the model. The probes are the small instruments on top of the vertical
tubes seen in figure 2 and are at about midheight of the model. In fig-
ure 5, stagnation temperature, obtained by averaging the results from
the two probes, is plotted against time for each test. Again the dashed
lines represent an average for the period during which test conditions
existed. The initial overshoot in temperature at about 1 second occurs
as the hot air which was stored in the heat exchanger prior to the test
passes out of the nozzle and past the stagnation temperature probes. As
before, in the case of model MW-4, values for only the first 6 seconds
were considered in averaging.

Mach number.- Calibration of the nozzle prior to the tests indicated
the Mach number to be 1.99 ± 0.02.

Angle of attack.- Models were mounted in the jet at an angle of attack
of 0°. An approximate check made from the pressure measurements on
model MW-7 indicated its angle of attack to be 0.1° counterclockwise,
looking down on the model in its test attitude. Similar calculations
could not be made for the other three models, since they contained no
pressure orifices.

Other aerodynamic data.- Additional aerodynamic data, computed from
the basic information given in the preceding sections, are compiled in
table 3. Average test conditions were used in these computations.

RESULTS AND DISCUSSION

A motion-picture film supplement has been prepared and is available
on loan. A request card form and a description of the film will be
found at the back of this paper, on the page immediately preceding the
abstract and index page.

At the beginning and end of a test, disturbances which are character-
istic of the test facility subject the model to random vibrations. These
disturbances occur chiefly during the period when the stagnation pressure
is below 50 lb/sq in. abs, while the flow over the model is subsonic and
very turbulent. As the stagnation pressure becomes larger, the distur-
bances decrease, and become small by the time test conditions are reached.
A more complete discussion of this phenomenon is given in the appendix of
reference 3.

Model Behavior

Model MW-4.- By 1.57 seconds after air began to flow, vibrations
had reduced until model MW-4 was virtually stationary. After this, no
motion of any consequence occurred until 5.22 seconds, when flutter of
the whole model, involving about $1\frac{1}{2}$ waves along the chord, started with
a frequency of about 240 cycles per second. During the time from
5.22 seconds to 5.25 seconds amplitudes increased and then remained sub-
stantially constant at the same frequency until 5.57 seconds. After
5.57 seconds, there was a rapid and continuing increase in amplitude,
with the chordwise bending distortions near the tip becoming very great.
Figure 6 shows several frames from high speed motion pictures taken
between 5.57 and 5.60 seconds. In these views, taken at 650 frames per
second, the distorted shape of the model is evident. It appears that
the chord was formed into about one and one-half waves, producing a flag-
waving effect. When amplitudes became sufficiently large, at 5.58 seconds,
the wing collapsed (as shown in fig. 6(c)) beginning near the tip at a
point about two-thirds of the chord downstream from the leading edge.
At this time the model tore away from the base, the tear being roughly
at the top of the doubler plate, beginning at the leading edge and pro-
gressing to the trailing edge. Failure was complete at 5.60 seconds.
Figure 7 shows the condition of the wing at the conclusion of the test.
Some of the distortion was due to collision with other objects after the
main portion of the model left the test stand, but much of the damage
resulted from action of the air during the test. Both the tip bulkhead
and the webs were crushed to some degree, and figure 7 shows that many
of the rivets failed.

The lighter tip bulkhead of model MW-4 (which was introduced in an
effort to permit freer expansion of the tip and thus, perhaps, to reduce
the tendency toward buckling in this region) was not effective in pre-
venting failure; in fact, this model failed earlier in the test period
than did model MW-2 with a thicker, stiffer tip bulkhead.

Since the model survived the air loads for several seconds, it is
not likely that they were the sole cause of failure. The temperatures

reached could cause a small reduction in strength, and Young's modulus could have been reduced by as much as about 10 percent.

The significant point observed in the tests of this and other models, however, is that flutter led to failure of the model. Thus, an attempt to find the cause of failure narrows down to finding why the models flutter. In references 5 to 7 attention has been called to the substantial loss of stiffness (with accompanying reduction in vibration frequency) which can be caused by thermal stress. In a previous section of this report, too, the flexibility of model MW-4, even at room temperature, was noted when it developed several natural modes of vibration not found in models MW-5, MW-6, or MW-7. The originally lower room-temperature stiffness plus the loss of stiffness due to thermal stress, together with the change in material properties, accounts for the flutter and failure of model MW-4.

Models MW-5 and MW-6.- No significant motion of either model MW-5 or MW-6 occurred except during the starting and shutdown periods, and both models appeared to be undamaged at the conclusion of the tests. The chordwise ribs in these models were an effective means of preventing flutter and failure, even in model MW-6 with a thinner skin than models MW-2, MW-4, or MW-5.

Model MW-7.- Model MW-7 apparently vibrated only during the starting and shutdown periods, and survived the test with only very minor damage. Slight buckles were noted on one skin near the root at the conclusion of the test, but were not apparent in the motion picture.

Model Temperatures

All model temperature data are listed in table 4. In all tests, temperatures were changing throughout, indicating that the entire test was transient in nature and of insufficient length to produce a steady-state temperature condition. Three temperature histories, typical of the test data, are shown in figure 8. Chordwise variation of skin temperature, at points unaffected by heat sinks, for model MW-6 is shown in figure 9; similar results were obtained for the other models. The temperature data show that heating of the model took place most rapidly near the leading edge and diminished steadily toward the trailing edge. Figure 10 shows the spanwise variation of skin temperature for model MW-7. The data indicate that, in the spanwise direction, heating took place more slowly near the root. Arrangement of instrumentation in other models did not permit similar comparisons, but such evidence as they do give indicates that figure 10 represents the usual spanwise temperature condition. Reduced temperatures near the root are due mainly to the lower stagnation temperature of the airstream near the boundary wall of the nozzle where the roots of the models were located, slightly accentuated, perhaps, by

the sink effect of the heavy lower bulkheads and root attachments. These
general characteristics of wing heating were borne out also by observing
colored motion-picture records of the models coated with thermal indicating
paints. Since the temperatures at which the paints changed color depended
upon the heating rate, they were not a very good indication of the actual
skin temperature, but did serve the purpose of telling whether one point
was hotter than another.

Figure 11 shows the temperature distribution in a skin and web com-
bination in the third bay from the leading edge of model MW-6 at 5 and
10 seconds after air began to flow from the nozzle. The general nature
of the distribution was typical of all of the other skin and web combi-
nations, and conformed to what was expected. Temperatures were highest
in the skin midway between webs. Transfer of heat from the skin increased
the web temperature, particularly in the vicinity of the flange and
decreased the skin temperature near the webs. Lowest temperature was in
the web midway between the skins.

Since the thermal stresses depend, in part, upon unequal temperature
distribution, such as that shown in figure 9, it is pertinent to note the
difference between skin and web temperatures for each of the models. For
all tests, the stagnation temperatures were very nearly the same (see
table 3) thus validating a direct comparison. Figure 12 shows the time
variation of the differences between the maximum skin temperature and the
minimum web temperature for the third skin and web element and indicates
that the greatest difference is only about 130° F for models MW-4 and MW-5
compared with 200° F for model MW-6 and 175° F for model MW-7. It appears
that the heavier skins of models MW-4 and MW-5 result in lower temperature
differences than those experienced by model MW-6 with a thinner skin,
although the temperature distribution may have been affected to some
extent by differences in joint conductivity. (See ref. 8.) The lower
value of thermal conductivity of the steel undoubtedly contributed to
lower interior (web) temperatures and thus to an increase in temperature
differences and to a later time at which the maximum temperature differ-
ence occurred in the test on model MW-7. Figure 12 shows that the alumi-
num models reached the point of maximum temperature difference in about 4
to 5 seconds, whereas the corresponding point for the steel model occurred
at about 7 seconds.

Calculated Skin Temperatures

Only the simplest skin-temperature calculations are included in this
report. No attempt has been made to compute temperatures in webs, ribs,
bulkheads, leading- and trailing-edge sections, or skin temperatures in
locations affected by other members which would introduce sink effects.
Thus, calculations have been made for skin temperatures only in locations
where one-dimensional analyses logically could be used.

Calculations were based upon average test conditions, which, for all practical purposes, existed except during the first 2 seconds. Zero time for the calculations was advanced slightly to compensate for the reduced heating effect during the first 2 seconds.

Skin-temperature calculations were made from equation (2) of reference 1:

$$T = T_{aw} - (T_{aw} - T_o)e^{-\frac{h(t - t_o)}{cw\tau}}$$

in which the subscript o refers to initial conditions. Values of T_{aw} used in the calculations were based on evaluation of the Prandtl number at adiabatic-wall temperatures, and heat-transfer coefficients were calculated by Van Driest's method with T equal to T_{aw}. Values of T_{aw} and h derived from the measured skin temperatures were compared with the calculated values. Heat-transfer coefficients were in good agreement, but the adiabatic-wall temperatures indicated by the test data were lower than those calculated. Some additional discussion of adiabatic-wall temperatures and heat-transfer coefficients is found in the appendix. Results are shown in figure 13, in which the calculated temperatures are seen to be generally a little higher than the test values, a condition directly attributable to the fact that calculated adiabatic-wall temperatures were higher than those indicated by experiment.

Strain-Gage Results

Strain gages were placed in all models (see table 1), but only those in model MW-4 were intended to provide stress information. In the remaining models the strain gages were used only to supply information concerning frequencies, and hence these latter gages were not calibrated for conversion of the data to stresses.

When the strain data for model MW-4 were converted to stresses, the results appeared to be incorrect, probably due in large part to the fact that the calibration of the gages was performed under conditions considerably different from those prevailing in the actual test. Consequently, no information on stresses has been included in this report.

Model Pressures

Test data for pressures in model MW-7 are given in table 5, except for orifices 2 and 3, which were omitted because usable data were not

obtained from them. Omission of values at occasional seconds means that
the record for that instrument was unreadable at the time indicated.
Such situations sometimes occur during the starting and shutdown periods
when very turbulent air is flowing over the model. Table 5 shows that
rather erratic pressures were measured during the first 2 seconds and
from 11 seconds on, which were the times of opening and closing of the
tunnel valve. Values listed for orifice 11 - 10 are differential pres-
sures between orifices 10 and 11; the negative sign indicates that ori-
fice number 10 was subjected to greater pressure than was orifice
number 11.

In general, pressures were above atmospheric pressure in the forward
part of the model, and below atmospheric pressure in the rearward part,
as would be expected. Orifices 6, 7, and 9 in the last bay downstream
were connected to miniature pressure pickups. Orifice number 8 was con-
nected to a recording manometer. The miniature gages measured pressures
considerably lower than did the gage at the same chordwise station which
was connected to the recording manometer. Some part of the discrepancy
may be due to tip effects, but this does not appear to account for all
of the difference.

Calculated Pressures

Pressures have been computed at points corresponding to those where
pressure measurements were obtained in model MW-7.

Basic pressures were calculated from equation (161) of reference 9
and corrected for tip effects where necessary in accordance with the
method of reference 10. The results at 5.0 seconds are compared with
test values in the following table. The time chosen has no special
significance; table 5 shows that the pressure fluctuated through a nar-
row range during the period of test conditions.

Orifice	Pressure, lb/sq in. abs	
	Computed	Measured
1	20.7	21.8
4	20.7	20.1
5	19.0	20.1
6	12.3	9.4
7	12.7	8.4
8	12.7	12.5
9	12.7	8.4
11	10.9	9.2

Agreement is fairly good for those orifices for which pressures were measured by the recording manometers (orifices 1, 4, 5, 8), but rather poor for those for which pressures were measured by the miniature gages. No explanation for this descrepancy between calculated and experimental results is known.

CONCLUSIONS

Four multiweb wing models were tested at 0° angle of attack, sea-level static pressure, a Mach number of 2, and a stagnation temperature of approximately 500° F, with the following results:

1. Temperature measurements appeared to give consistent and reasonably accurate results; measured skin temperatures agreed fairly well with calculated values.

2. Heat-transfer coefficients derived from the measured skin temperatures were generally in good agreement with those calculated by the method of Van Driest, but adiabatic-wall temperatures were lower than indicated by theory.

3. Model static pressures measured by recording manometers agreed fairly well with computed values; those which were measured by NACA miniature electrical pressure gages did not agree very well with other test results or with calculated values.

4. The lightweight tip bulkhead of model MW-4 was ineffective in preventing flutter and failure; the model seemed to be less stable than was model MW-2 with a more nearly rigid tip bulkhead.

5. The addition of chordwise ribs in model MW-5 was an effective means of preventing flutter, and even with a thinner skin, as in model MW-6, the chordwise ribs were sufficient to attain stability.

6. The steel material used for model MW-7 permitted it to survive, although it showed evidence of damage in the form of slight permanent skin buckles near the root.

7. The flutter and failure of model MW-4 was due to loss of stiffness caused by thermal stresses and change in material properties resulting from aerodynamic heating.

Langley Aeronautical Laboratory,
     National Advisory Committee for Aeronautics,
          Langley Field, Va., July 17, 1957.

APPENDIX

CALCULATION OF ADIABATIC-WALL TEMPERATURE

AND HEAT-TRANSFER COEFFICIENTS

Since the tests discussed in the present paper were necessarily too short to reach steady-state temperature conditions, the adiabatic-wall temperatures and heat-transfer coefficients could be determined only by calculation. The formula used for calculating adiabatic-wall temperature was

$$T_{aw} = T_\infty + \eta_r\left(T_s - T_\infty\right)$$

as given in reference 11 (temperatures are in absolute units). The recovery factor may be based upon evaluation of the Prandtl number at any temperature between free-stream and adiabatic-wall temperatures; however, for these tests T_{aw} varies only a few degrees no matter what temperature is chosen within this range. The calculated values shown in figure 14 are based upon Prandtl numbers evaluated at the adiabatic-wall temperature. The relationship between the recovery factor and the Prandtl number depends upon whether the air flowing over the model is laminar or turbulent. Reynolds numbers of 3×10^6 and higher at points where skin thermocouples were located probably indicate turbulent flow, and the calculations have been based upon turbulent flow conditions, with $\eta_r = N_{Pr}{}^{1/3}$.

Heat-transfer coefficients were calculated in three ways: (1) from the method of Colburn as applied by Chauvin and deMoraes in reference 12, using parameters based upon local flow conditions just outside the boundary layer, (2) Eckert's method as given in reference 13, with parameters based on a reference temperature, and (3) by Van Driest's method of reference 14.

In all cases, local flow conditions were calculated by a shock-expansion analysis of two-dimensional flow around a circular-arc airfoil. In methods (2) and (3), skin temperatures were taken first as equal to local stream temperatures and then as equal to the adiabatic-wall temperature, thus forming bands within which the theoretical values of h lie. Comparisons of calculated T_{aw} and h with "indicated" test values are shown in figure 14. "Indicated" values were obtained from the various skin temperature histories through use of the differential equation of heat transfer to the skin which may be written

$$T = - \frac{c_W\tau}{h} \frac{dT}{dt} + T_{aw}$$

in which $c_W\tau$ is the heat capacity of the skin per unit area. If $c_W\tau/h$ and T_{aw} are considered to be constants, the equation is that of a straight line having the slope $- \frac{c_W\tau}{h}$ and an intercept on the T-axis of T_{aw}. Values of T and dT/dt were determined at several points along a given curve of temperature history and plotted with T as ordinate and dT/dt as abscissa. Then a straight line was passed through these points by the method of least squares. The slope and intercept of such a line determined "indicated" values of h and T_{aw}. The assumption that h at a given point is invariant with time is, of course, not quite true. Changing skin temperature from beginning to end of the test causes h to vary through the bands which are shown in figure 14, but the error due to assuming constant h is small and the simplification seems justified. In most cases, computed adiabatic-wall temperatures were a little higher than were those obtained from the test results, which may be due to some uncertainty about the test stagnation tempera-ture. (A short discussion of the difficulty of finding the true stagna-tion temperature is given in the appendix of ref. 3.) Heat-transfer coefficients as computed by the Colburn method were considerably higher than those indicated by test results, but values calculated by Eckert's or Van Driest's methods compared quite well with the "indicated" values from the tests.

Heat-transfer coefficients and model temperatures may have been affected slightly by the layer of paint on the model surfaces. A cor-rected heat-transfer coefficient h' may be calculated from the expression

$$h' = \frac{h}{1 + h \frac{L}{k}}$$

in which L is the thickness of the paint in feet and k is the thermal conductivity of the paint in $Btu/(ft)(sec)(^{\circ}F)$. Since a coating of only about 0.002-inch thickness was applied to the models, it might be expected that h was not seriously reduced. Reference 15 discusses the insu-lating properties of several paint finishes, and indicates that for thin coatings, the temperature histories are only slightly affected. (See, for instance, figure 15 of ref. 15.)

REFERENCES
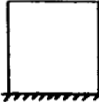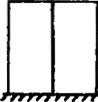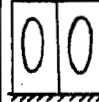
1. Heldenfels, Richard R., Rosecrans, Richard, and Griffith, George E.: Test of an Aerodynamically Heated Multiweb Wing Structure (MW-1) in a Free Jet at Mach Number 2. NACA RM L53E27, 1953.

2. Heldenfels, Richard R., and Rosecrans, Richard: Preliminary Results of Supersonic-Jet Tests of Simplified Wing Structures. NACA RM L53E26a, 1953.

3. Griffith, George E., Miltonberger, Georgene H., and Rosecrans, Richard: Tests of Aerodynamically Heated Multiweb Wing Structures in a Free Jet at Mach Number 2 - Two Aluminum-Alloy Models of 20-Inch Chord With 0.064- and 0.081-Inch-Thick Skin. NACA RM L55F13, 1955.

4. Patterson, John L.: A Miniature Electrical Pressure Gage Utilizing a Stretched Flat Diaphragm. NACA TN 2659, 1952.

5. Budiansky, Bernard, and Mayers, J.: Influence of Aerodynamic Heating on the Effective Torsional Stiffness of Thin Wings. Jour. Aero. Sci., Vol. 23, no. 12, Dec. 1956, pp. 1081-1093, 1108.

6. Dryden, Hugh L., and Duberg, John E.: Aeroelastic Effects of Aerodynamic Heating. Proc. of Fifth AGARD General Assembly (Canada), June 15-16, 1955, pp. 102-107.

7. Vosteen, Louis F., and Fuller, Kenneth E.: Behavior of a Cantilever Plate Under Rapid Heating Conditions. NACA RM L55E20c, 1955.

8. Brooks, William A., Jr., Griffith, George E., and Strass, H. Kurt: Two Factors Influencing Temperature Distributions and Thermal Stresses in Structures. NACA TN 4052, 1957.

9. The Staff of the Ames 1- by 3-Foot Supersonic Wind-Tunnel Section: Notes and Tables for Use in the Analysis of Supersonic Flow. NACA TN 1428, 1947.

10. Czarnecki, K. R., and Mueller, James N.: An Approximate Method of Calculating Pressures in the Tip Region of a Rectangular Wing of Circular-Arc Section at Supersonic Speeds. NACA TN 2211, 1950.

11. Hilsenrath, Joseph: The NBS-NACA Tables of Thermal Properties of Gases. Table 2.44 Dry Air - Prandtl Number. National Bur. Standards, U.S. Dept. of Commerce, July 1950.

12. Chauvin, Leo T., and deMoraes, Carlos A.: Correlation of Supersonic
    Convective Heat-Transfer Coefficients From Measurements of the Skin
    Temperature of a Parabolic Body of Revolution (NACA RM-10). NACA
    TN 3623, 1956. (Supersedes NACA RM L51A18.)

13. Eckert, Ernst R. G.: Survey on Heat Transfer at High Speeds. WADC
    Tech. Rep. 54-70, Wright Air Dev. Center, U.S. Air Force, Apr.
    1954.

14. Van Driest, E. R.: Turbulent Boundary Layer in Compressible Fluids.
    Jour. Aero. Sci., vol. 18, no. 3, Mar. 1951, pp. 145-160, 216.

15. Smith, W. A., and Kops, E. A.: Heat Insulation Effectivity of
    Selected Paint Finishes Investigation of Model General.
    Rep. No. 8675 (Contract No. AF33(600)-5942), Convair, Sept. 22,
    1954.

TABLE 1.- MODEL INSTRUMENTATION

Instrument	Model			
	MW-4	MW-5	MW-6	MW-7
Thermocouples	27	24	24	24
Strain gages	17	6	6	6
Pressure gages:				
Miniature -				
Total				4
Differential				1
Manometer -				
Total				4
Differential				1

TABLE 2.- VIBRATION CHARACTERISTICS

Model	Frequency, cps, for node line[a] -										
	A	B	C	C_1	D	E	F	G	H	I	J
MW-2	62	141	260	---	332	393	441	526	587	665	703
MW-4	71	149	277	---	348	392	430	533	476	661	715
MW-5	63	151	---	297	445	582	---	---	---	---	---
MW-6	65	141	---	302	427	567	---	---	---	---	---
MW-7	60	136	238	---	316	364	---	452	---	---	---

[a]Modes shown are composites from modes for all models. Individual modes varied slightly from those shown.

TABLE 3.- AERODYNAMIC TEST DATA

Model	Mach number	Stagnation pressure, lb/sq in. abs	Stag-nation tempera-ture °F	Free-stream static pressure lb/sq in. abs	Free-stream dynamic pressure, lb/sq in.	Free-stream tempera-ture, °F	Free-stream velocity, ft/sec	Free-stream density, slugs/ft^3	Speed of sound, ft/sec	Reynolds number per ft, 1/ft
MW-4	1.99	121	491	15.7	43.5	71	2.25×10^3	2.48×10^{-3}	1.13×10^3	14.7×10^6
MW-5	1.99	119	500	15.4	42.7	76	2.27	2.41	1.14	14.2
MW-6	1.99	112	499	14.5	40.2	75	2.25	2.27	1.14	13.3
MW-7	1.99	118	497	15.3	42.4	74	2.25	2.40	1.14	14.1

TABLE 4.- MODEL TEMPERATURES

Time, sec	Temperature, °F, at thermocouple[a] -																									
	1	2	3	4	5	6	7	8	9	10	11	12	13	14	15	16	17	18	19	20	21	22	23	24	25	26
Model MW-4																										
0	59	59	58	58	58	58	58	58	58			56	57	58	58	58	58	57	58	58	57		56	61	59	60
1	73	60	103	94	100	97	96	91	92			69	99	92	97	88	94	91	85	90	58		57	139	112	153
2	140	80	175	154	168	164	161	152	153			115	166	149	154	140	155	143	134	157	75		69	257	224	286
3	226	119	243	221	230	225	219	204	200			159	230	204	200	185	205	187	173	195	122		96	305	280	319
4	290	171	291	270	276	270	263	246	237			196	278	244	236	220	246	224	208	227	167		134	304	317	350
5	336	221	328	308	314	308	300	282	271			223	318	277		247	281	258	238	256	215		175	351	347	367
Model MW-5																										
0	51	51		51	50	51	51	50	50	49	49	49	51	50	51	51	51	52	49	48	48	49	49	49		
1	98	93		89	91	90	89	76	86	83	85	83	83	82	86	52	51	55	49	48	50	52	46	57		
2	173	160		154	156	146	147	127	137	136	141	144	142	143	150	68	65	78	65	63	61	64	57	90		
3	245	226		214	219	199	201	179	187	188	192	197	191	188	191	99	93	116	95	93	85	88	78	126		
4	291	274		259	265	241	243	221	228	230	234	240	229	223	222	136	129	154	131	133	117	114	113	161		
5	325	311		291	300	277	277	258	263	266	268	275	264	253	249	173	160	192	169	174	154	150	153	193		
6	351	338		316	327	306	306	287	291	293	295	302	287	278	271	211	199	225	204	213	192	184	191	221		
7	372	362		336	348	329	327	310	314	316	318	323	310	299	292	244	231	256	236	249	223	216	224	246		
8	390	378		352	366	349	345	329	335	335	336	340	327	316	308	274	259	283	264	275	254	244	255	268		
9	403	393		365	380	364	361	346	351	350	353	354	342	331	323	299	286	305	289	304	281	271	282	290		
10	412	403		374	390	377	374	360	365	364	365	366	355	343	337	320	306	323	310	326	304	295	305	309		
11	420	411		381	398	387	384	371	376	374	376	375	365	354	348	339	322	337	327	344	325	314	324	325		
12	424	416		385	404	395	392	380	385	381	382	382	373	366	362	354	338	350	341	359	341	331	341	338		
13	428	420		388	408	398	396	387	390	382	384	384	376	380	378	369	351	363	351	369	355	346	355	352		
14	430	420		387	409	403	401	391	395	389	391	390	385	379	384	371	355		355	364	360	355	348	356		
15	428	419		389	410	403	400	393	394	390	391	391	385	382	382	375	368		363	365	361	363	361	360		

[a]Where data for a particular thermocouple are not given, thermocouple was not in proper working condition at time of test. Where data are listed for only part of test, values beyond those given were considered unreliable.

TABLE 4.- MODEL TEMPERATURES - Concluded

Time, sec	Temperature, °F, at thermocouple[a] -																							
	1	2	3	4	5	6	7	8	9	10	11	12	13	14	15	16	17	18	19	20	21	22	23	24
Model MW-6																								
0	56	55		56	56	54	56	57	57	57	57	57	57	58	57	58	56	58	57	57	57	57	57	57
1	118	113		108	111	101	102	110	97	96	102	103	100	105	105	60	58	63	60	59	57	59	59	66
2	209	192		182	186	165	169	186	159	159	167	178	170	178	183	83	67	85	76	77	68	74	77	96
3	284	262		247	252	223	226	249	212	216	223	238	228	232	230	124	79	119	105	109	92	101	108	131
4	332	309		291	298	265	268	295	253	259	265	281	271	271	264	173	99	159	144	153	126	137	149	166
5	364	343		322	332	298	301	327	285	292	297	316	302	302	292	218	124	198	183	195	162	174	191	197
6	386	367		342	355	326	328	352	313	319	323	338	328	327	315	257	150	232	220	235	199	209	230	226
7	401	387		358	373	348	350	372	335	340	344	358	348	347	334	290	178	264	252	269	221	243	262	251
8	417	402		371	390	365	367	386	354	358	361	374	364	363	351	318	205	291	281	299	265	273	291	274
9	425	412		380	400	381	382	398	370	373	375	385	377	377	365	341	232	315	307	325	293	299	316	295
10	432	421		388	409	392	393	408	382	383	387	396	387	387	376	360	256	335	328	342	317	322	337	313
11	438	429		394	419	402	402	414	392	394	396	403	395	395	385	375	276	349	346	359	337	341	352	327
12	441	433		397	422	410	410	421	401	401	402	409	401	402	393	382	298	365	361	373	356	358	368	342
13	445	437		401	427	416	414	423	407	408	409	415	408	407	398	397	313	372	373	377	370	372	376	357
14	445	438		401	430	420	419	426	412	411	413	417	410	411	406	407	328	373	381	391	378	378	384	368
15	446	439		402	431	422	421	428	415	413	415	420	413	417	416	412	341	376	392	402	382	381	397	377
16	446	440		402	432	424	424	429	417	417	417	421	415	420	418	416	351	378	402	409	383	387	404	386
17	444	438		400	431	425	423	429	418	419	419	410	420	421	418	417	360	379	405	412	388	394	409	384
Model MW-7																								
0	51	50		50	50	48	49	54	53	59	59	59	58	47	62	60	61	62	58	56	60	56	60	61
1	66	52		90	91	85	85	85	81	89	90	89	60	54	94	98	98	96	61	59	86	58	60	64
2	120	65		152	157	143	144	137	128	146	145	145	69	77	162	161	163	153	71	63	129	63	65	78
3	187	88		206	217	193	197	187	171	197	197	188	86	107	224	221	215	204	95	75	176	77	74	98
4	249	120		258	264	229	241	226	211	241	228	222	104	137	274	271	258	244	128	95	215	96	91	119
5	297	156		301	302	263	277	260	242	275	259	252	122	166	311	308	290	274	161	117	247	116	110	139
6	334	189		333	331	293	306	289	268	303	285	278	141	191	341	339	316	298	196	142	276	139	133	158
7	363	221		356	354	327	313	313	293	327	308	299	160	213	367	362	336	316	229	167	299	161	153	177
8	383	247		371	370	352	347	331	310	346	327	317	176	235	384	381	351	330	260	193	320	185	176	189
9	400	273		385	386	372	363	349	329	363	344	333	194	252	400	397	363	342	287	216	337	205	196	211
10	411	296		394	396	383	375	362	341	374	356	345	209	267	409	407	372	349	312	239	351	226	215	226
11	420	316		403	403	394	384	374	353	385	364	355	225	281	418	414	377	353	332	261	362	246	234	241
12	425	332		408	409	404	391	381	363	392	375	366	238	294	423	420	384	357	350	282	371	263	253	255
13	427	345		413	412	409	397	387	370	395	382	373	248	310	424	421	385	354	355	298	378	281	271	268
14	427	357		414	414	413	398	391	375	398	383	377	265	318	416	424	386	353	366	315	383	298	287	275
15	425	363		414	413	413	399	390	374	398	384	376	273	324	414	424	384	352						

[a]Where data for a particular thermocouple are not given, thermocouple was not in proper working condition at time of test. Where data are listed for only part of test, values beyond those given were considered unreliable.

TABLE 5.- PRESSURES FOR MODEL MW-7

Time, sec	Pressure, lb/sq in. abs, at orifice[a] -								
	1	4	5	6	7	8	9	11 - 10	11
0	14.9	14.9	14.9	14.9	14.9	14.9	14.9	-0.09	14.9
1	21.1	18.3	20.7	7.9	7.2	16.8	9.8		16.1
2	20.2	18.7	19.3	9.4	8.4	12.4	8.5	-.97	9.3
3	21.7	20.1	20.2	9.4	8.4	12.5	8.5	-.98	9.2
4	22.2	20.6	20.6	9.6	8.6	12.8	8.8	-1.05	9.3
5	21.8	20.1	20.1	9.4	8.4	12.5	8.4	-1.09	9.2
6	22.3	20.6	20.7	9.7	8.6	12.9	8.7	-1.33	9.4
7	21.9	20.3	20.3	9.5	8.5	12.6	8.4	-1.55	9.2
8	21.9	20.1	20.1	9.4	8.3	12.5	8.3	-2.34	9.1
9	21.3	19.7	19.7	9.2	8.1	12.3	8.2	-2.56	10.5
10	20.5	18.8	18.7	9.2	7.5	11.9	7.7	-.49	16.4
11	18.9	17.3	16.8	9.2	6.5	12.6	9.0	-2.31	13.9
12	15.7	14.3	13.9	19.5	17.6	16.5	11.8		25.3
13	21.0	16.0	20.6	(a)		13.5			19.2
14	15.1	14.9	14.9	12.4	12.4	14.9	9.9	.05	15.2

[a]Omissions from table indicate that test record could not be read at that time.
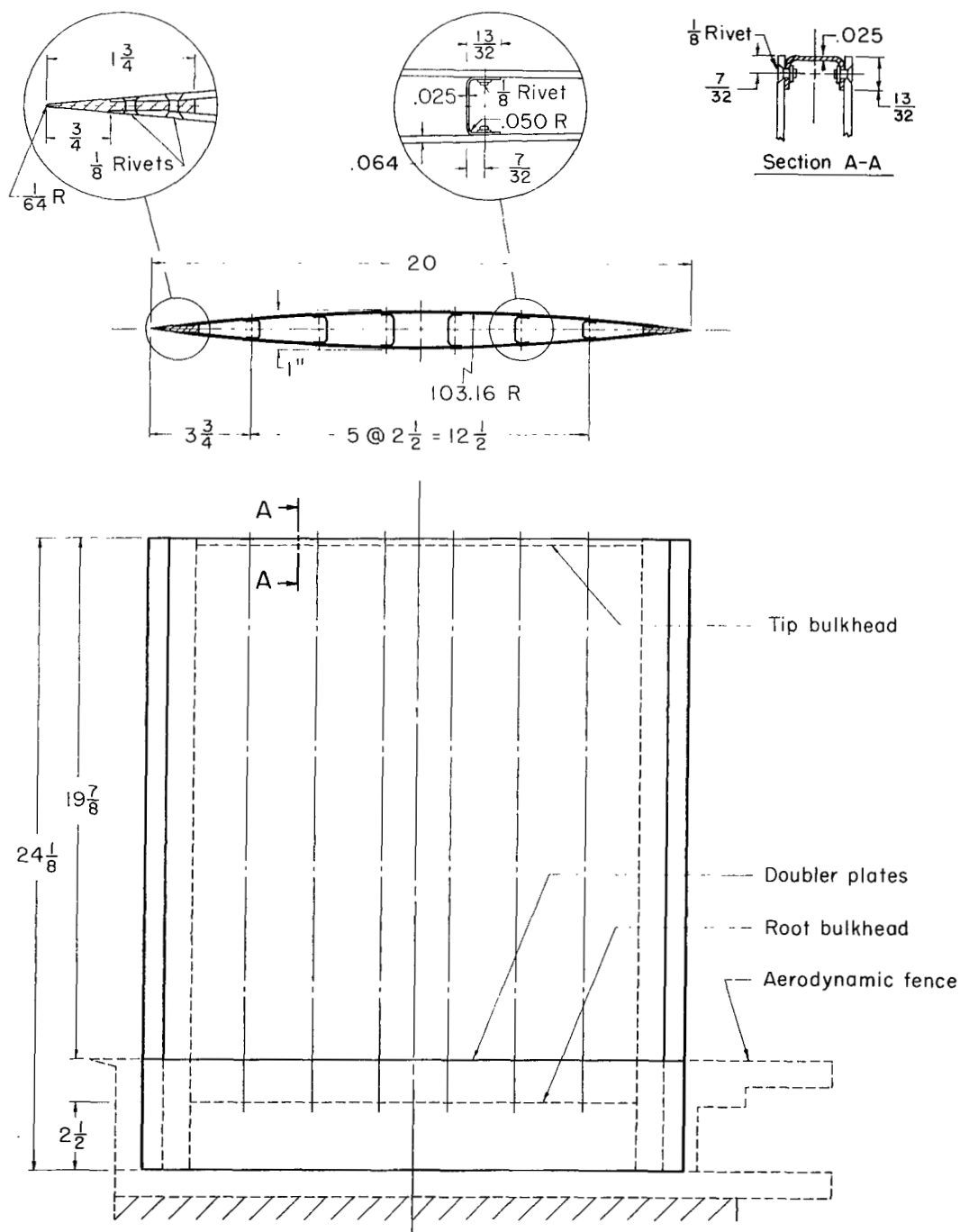
(a) Model MW-4.

Figure 1.- Details of model construction.
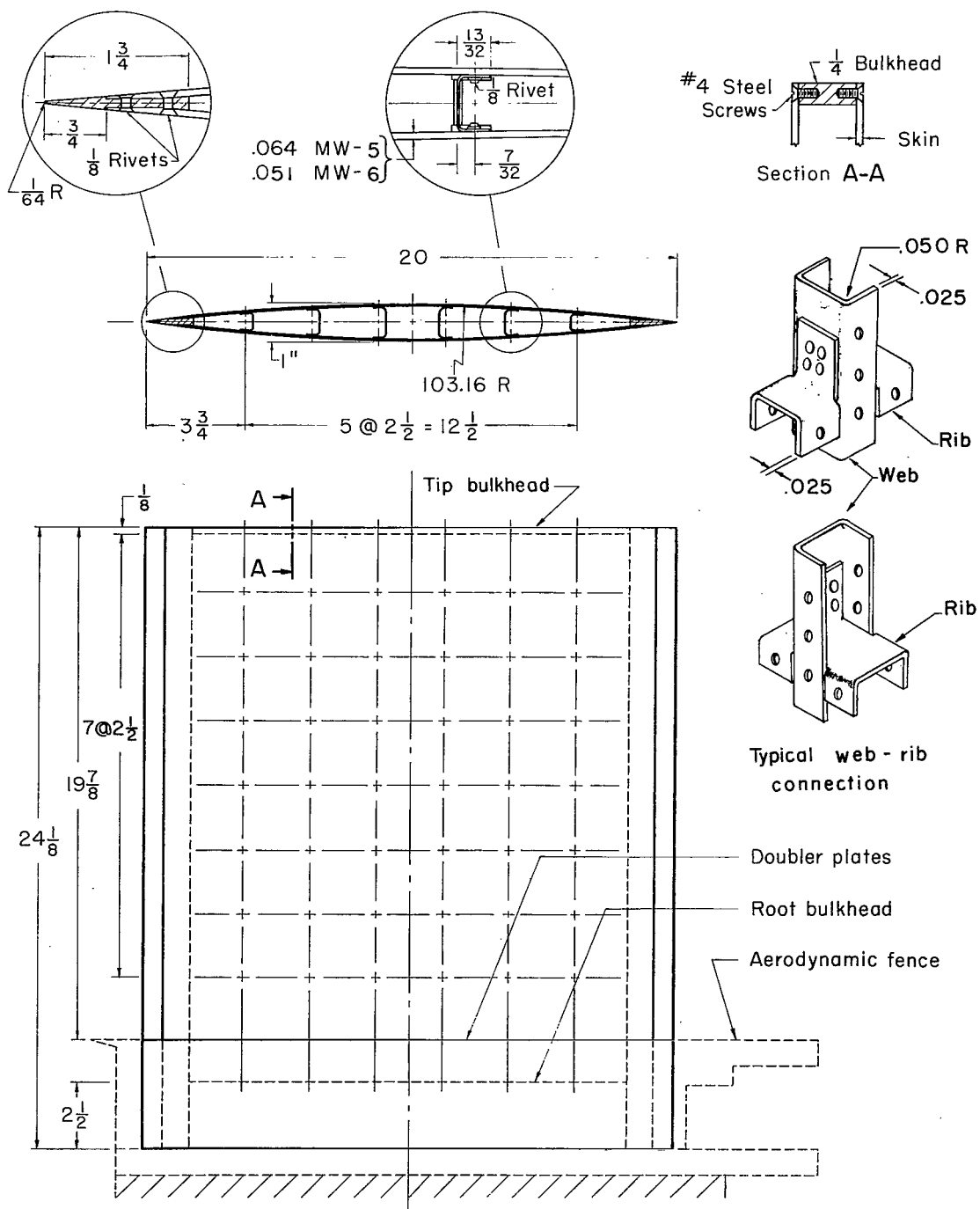
(b) Models MW-5 and MW-6.

Figure 1.- Continued.
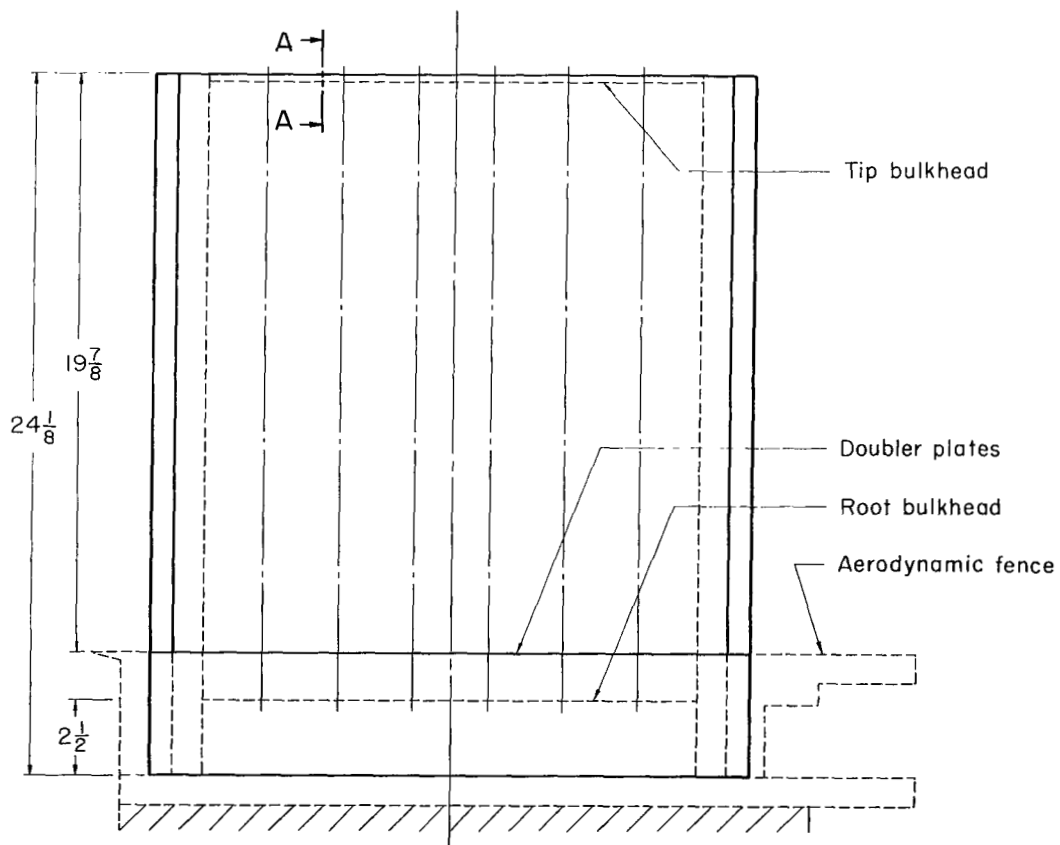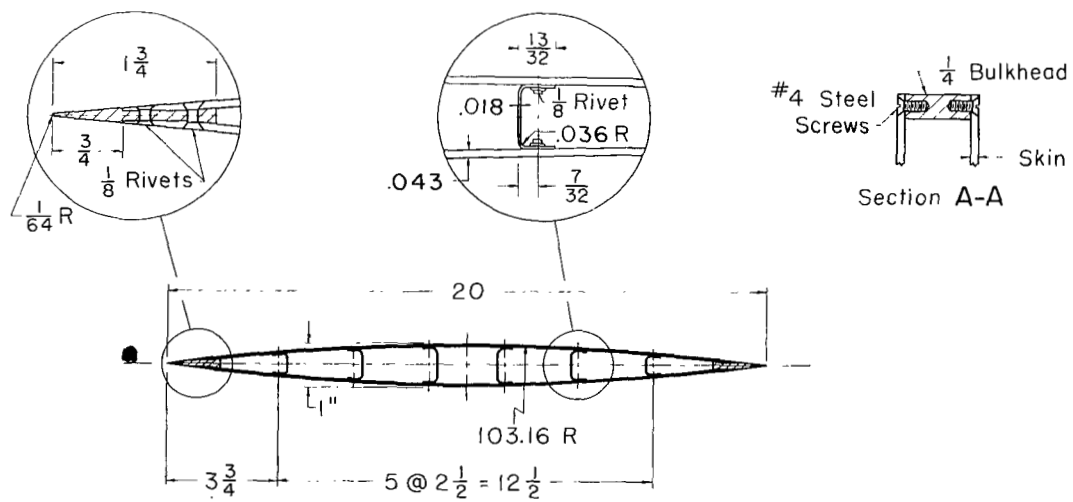
(c) Model MW-7.

Figure 1.- Concluded.
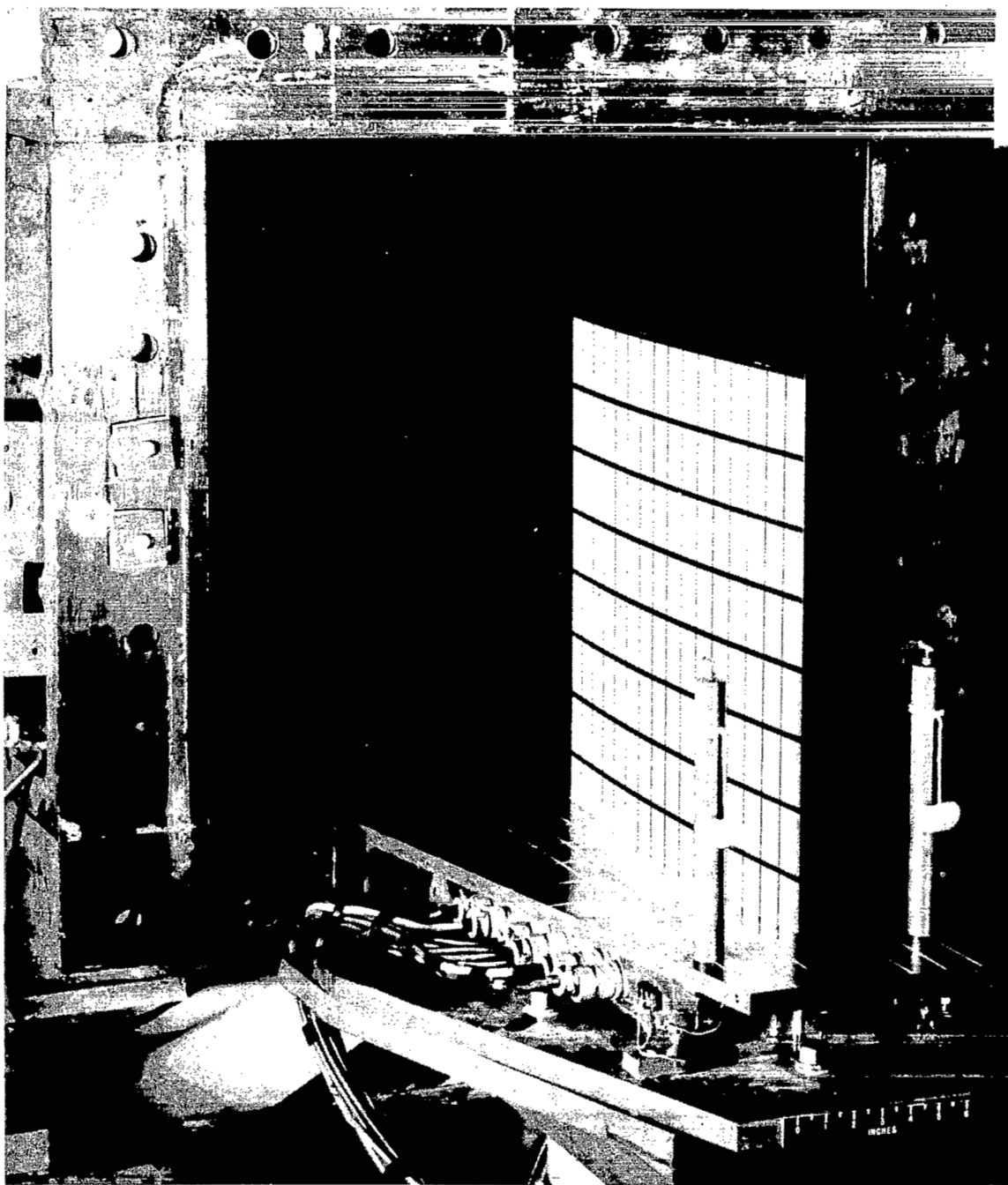
L-81922

Figure 2.- Standard grid paint pattern used on one side of models MW-4 and MW-7 and on both sides of models MW-5 and MW-6.
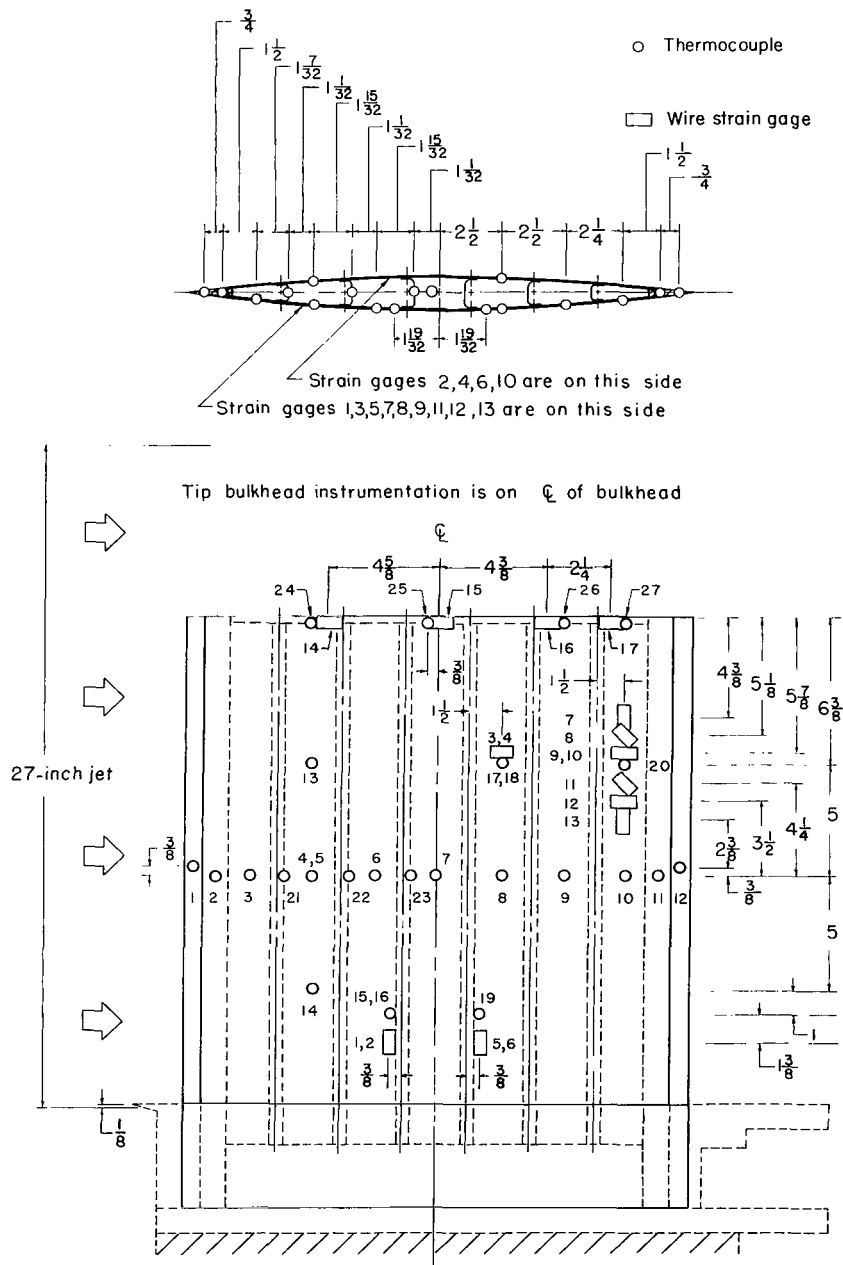
(a) Model MW-4.

Figure 3.- Location of instrumentation.

(b) Models MW-5 and MW-6.

Figure 3.- Continued.
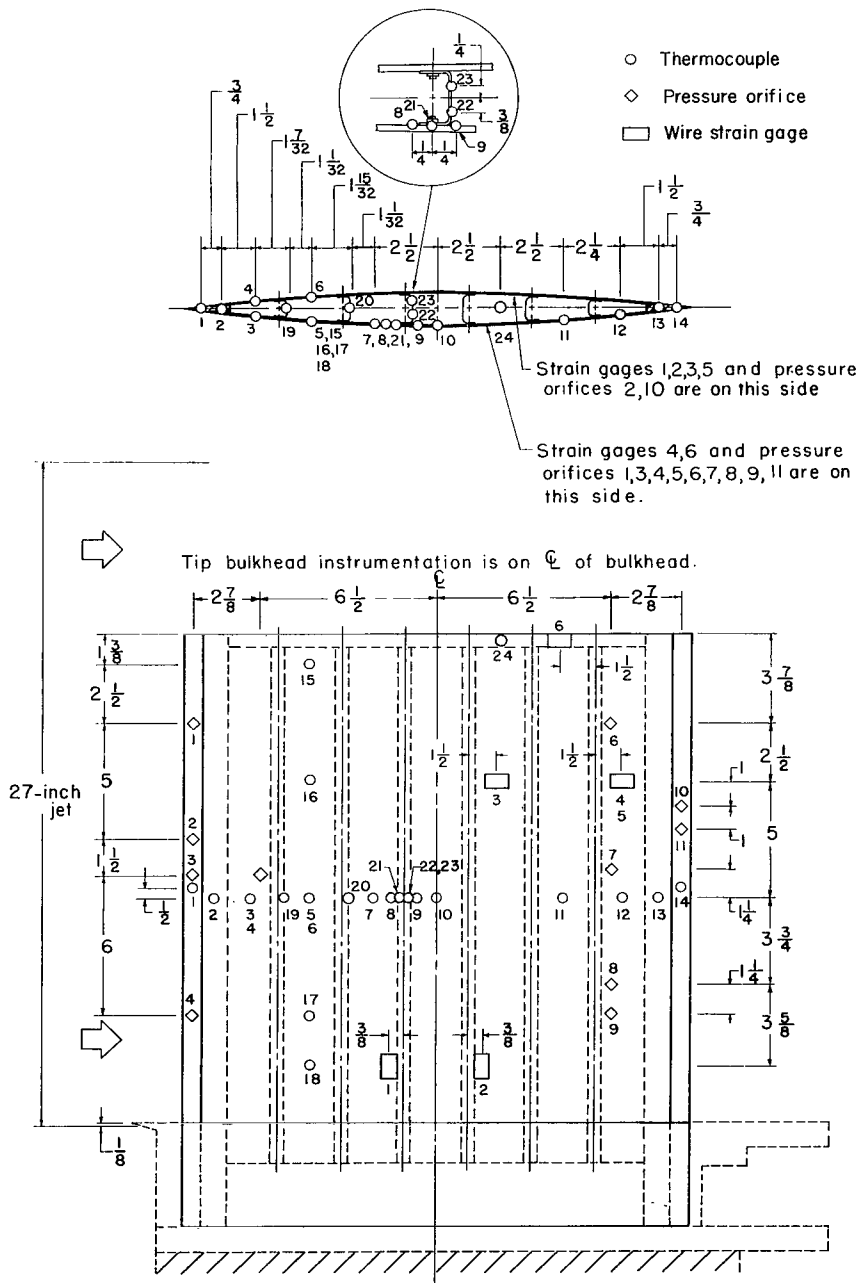
(c) Model MW-7.

Figure 3.- Concluded.
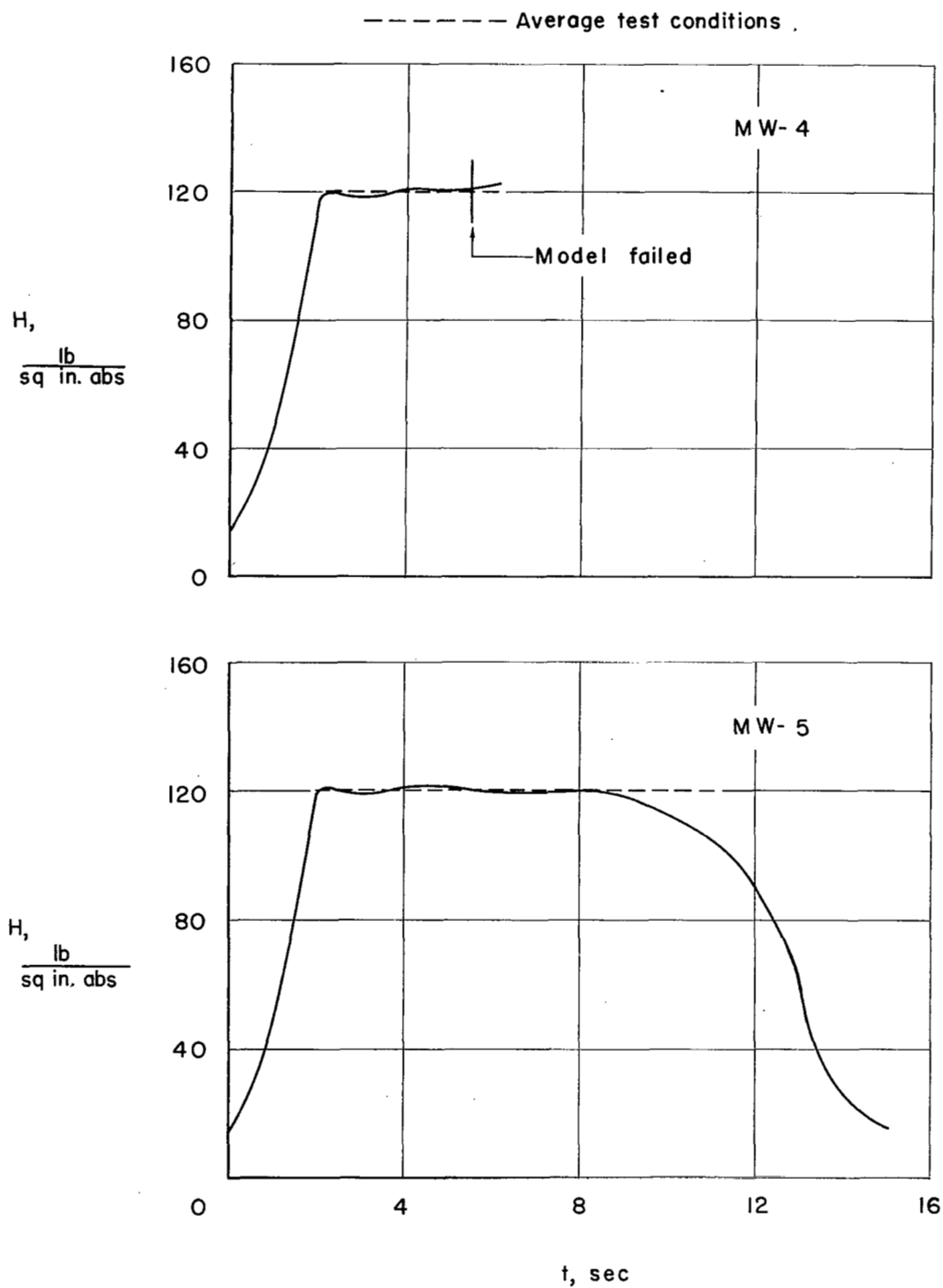
Figure 4.- Stagnation pressures.
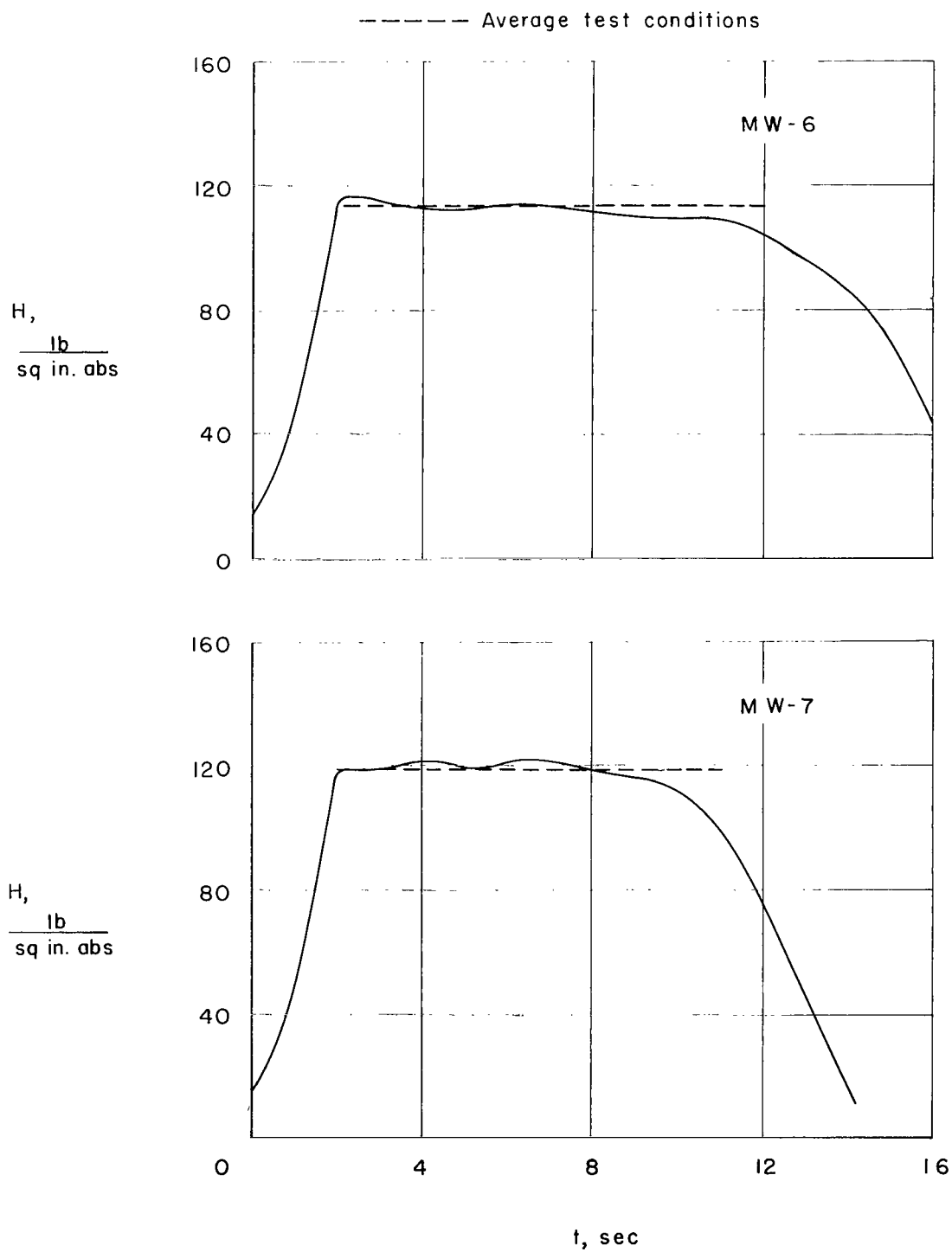
Figure 4.- Concluded.
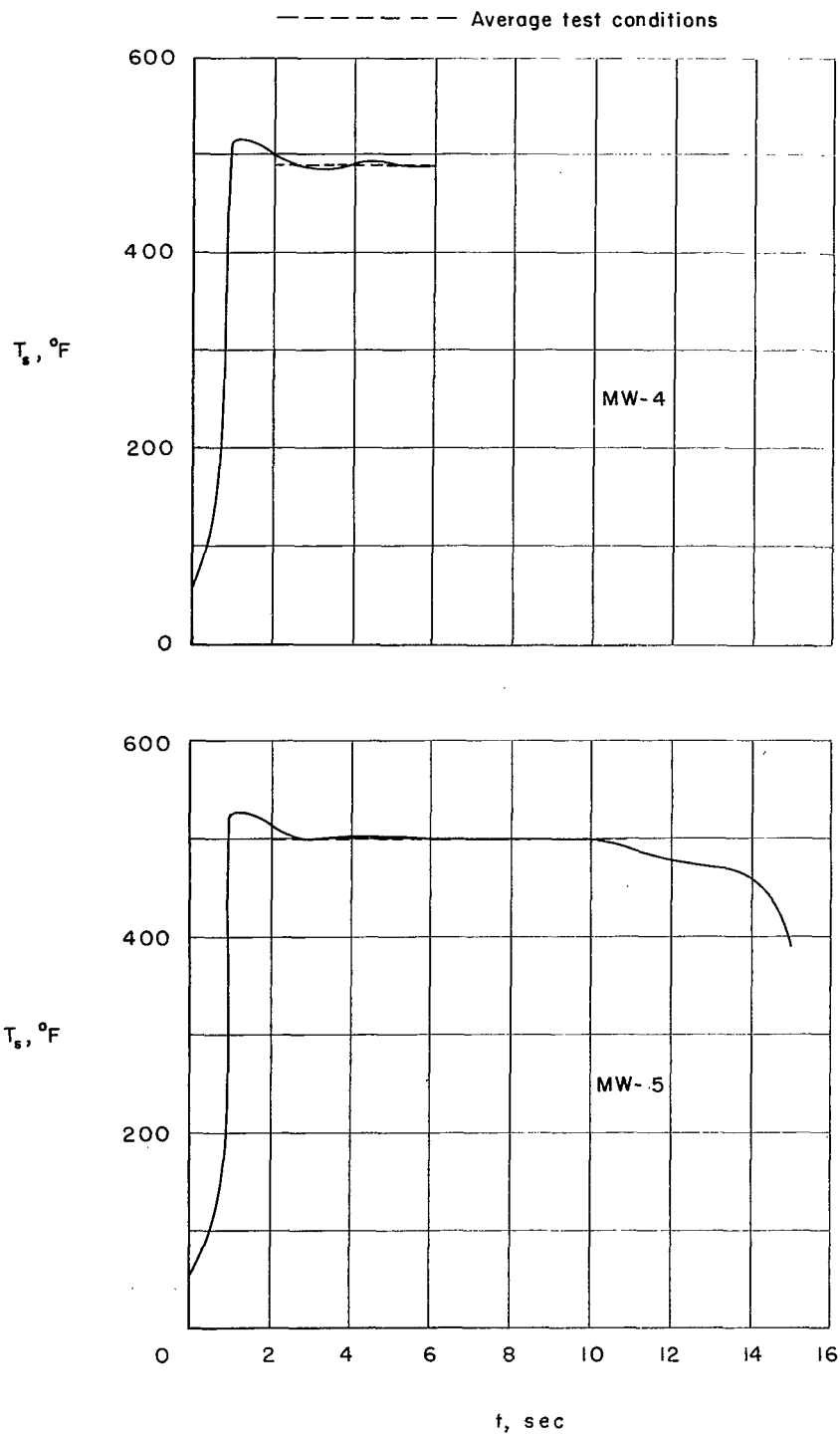
Figure 5.- Stagnation temperatures.
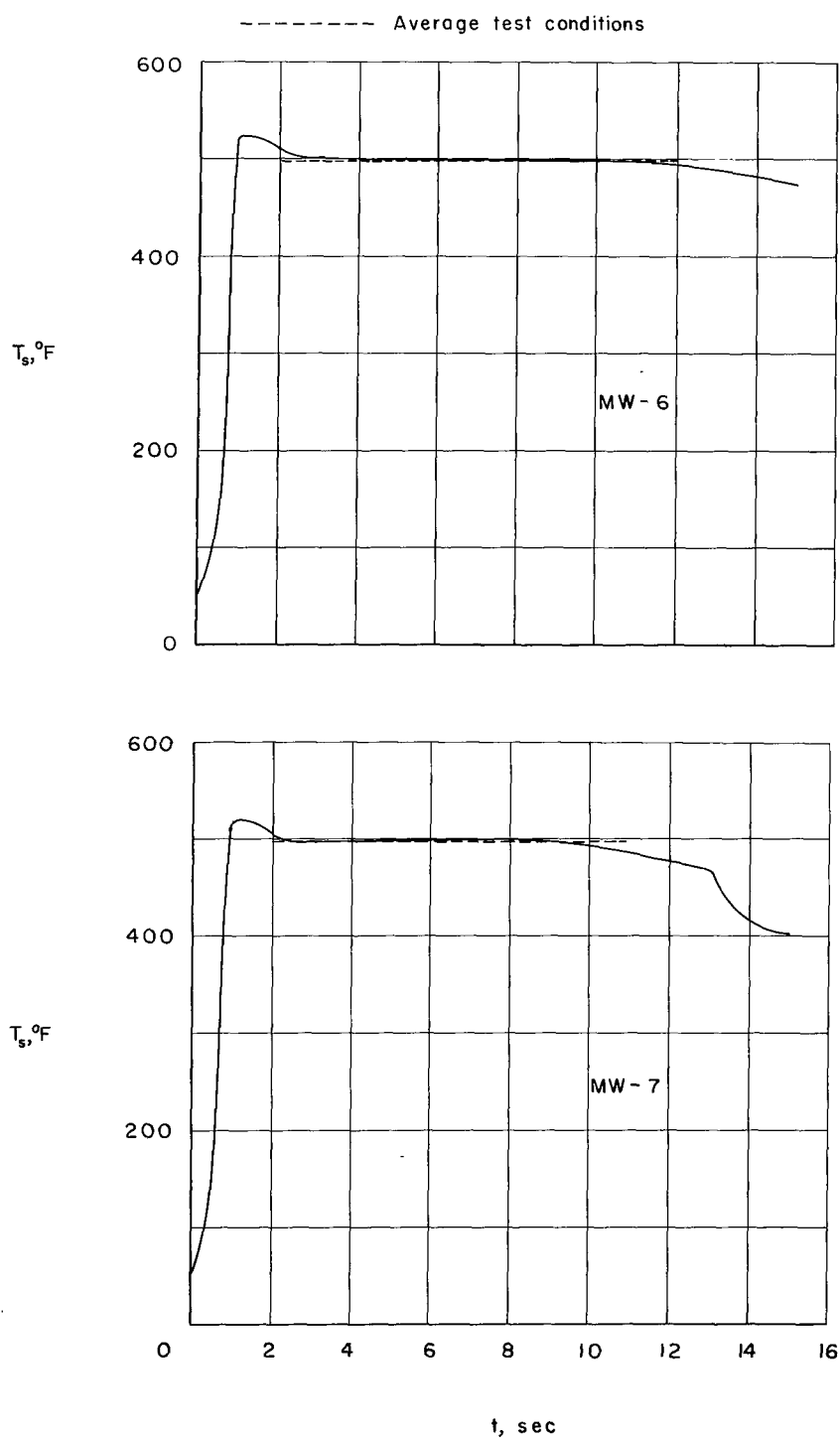
Figure 5.- Concluded.
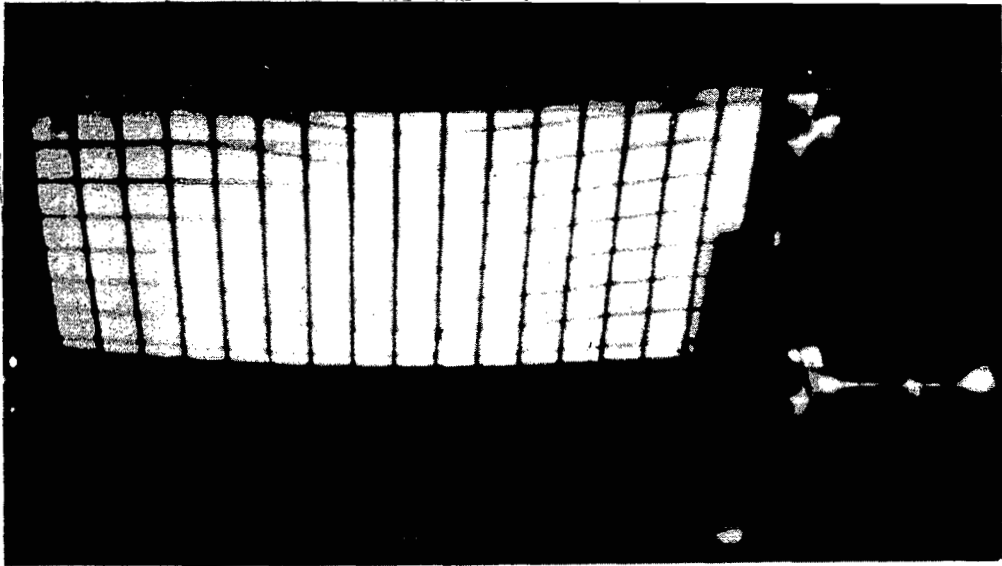
5.572 seconds
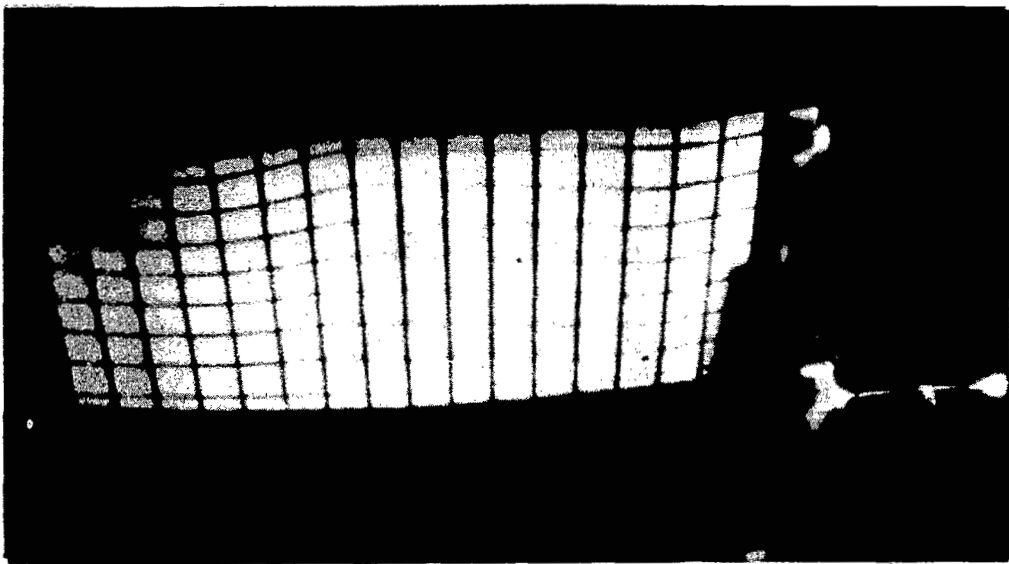
5.574 seconds   L-57-2721

(a) Small amplitude.

Figure 6.- Flutter of model MW-4.
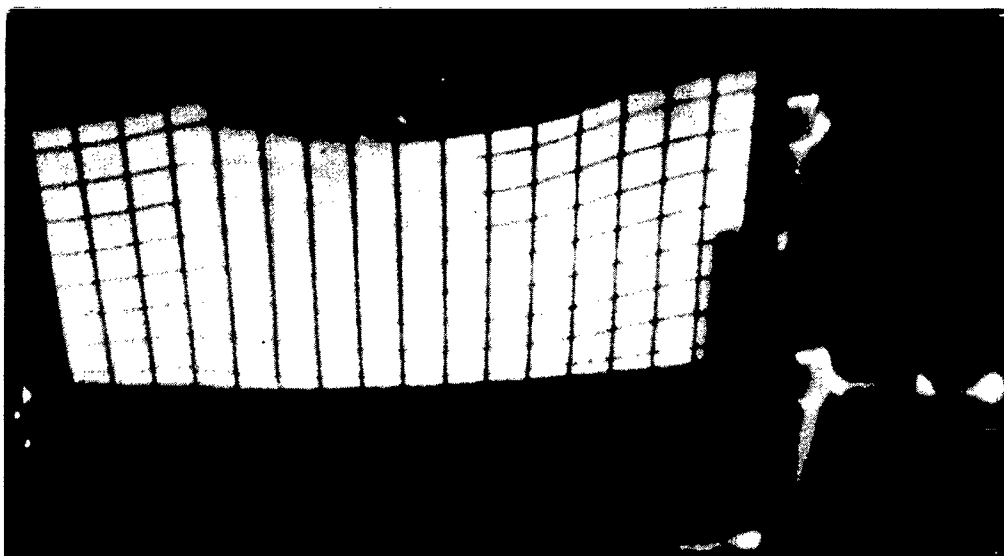
5.577 seconds
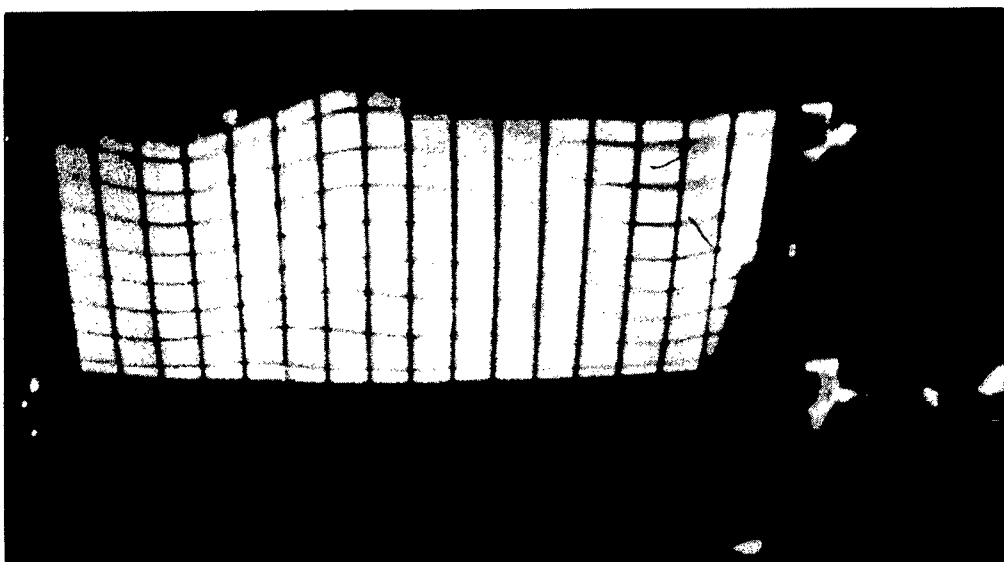
5.578 seconds   L-57-2722

(b) Amplitude near failure.

Figure 6.- Continued.
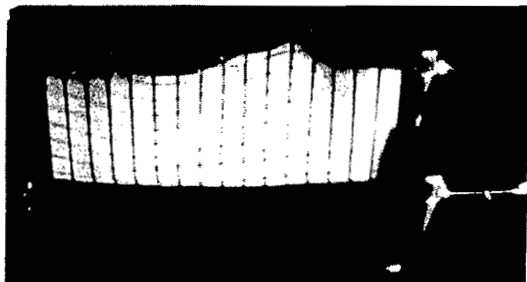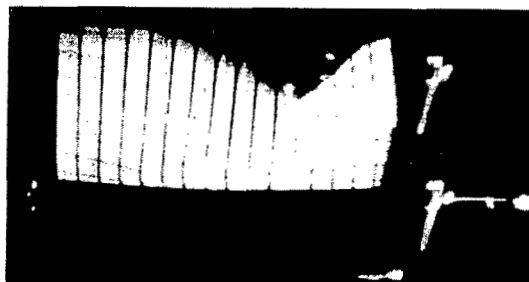
5.580 seconds   5.583 seconds
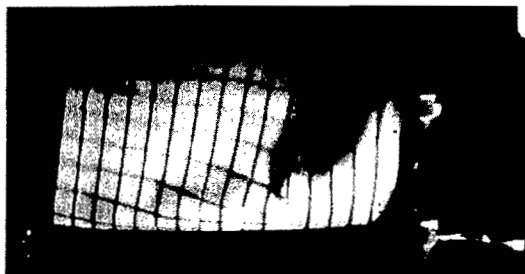
5.586 seconds   5.589 seconds

5.592 seconds   5.595 seconds

(c) Failure sequence.   L-57-2723

Figure 6.- Concluded.
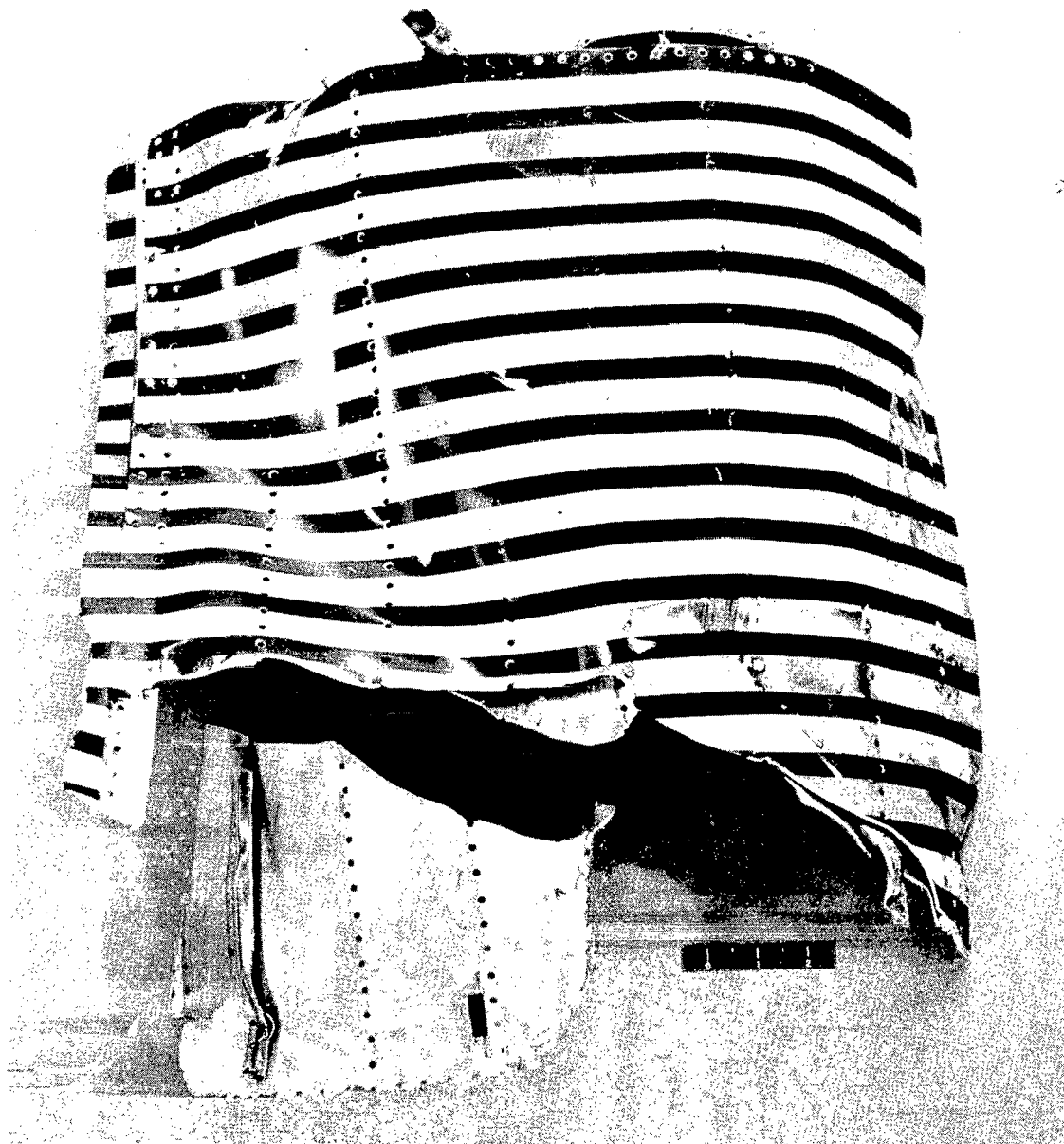
Figure 7.- Model MW-4 after failure.   L-78913
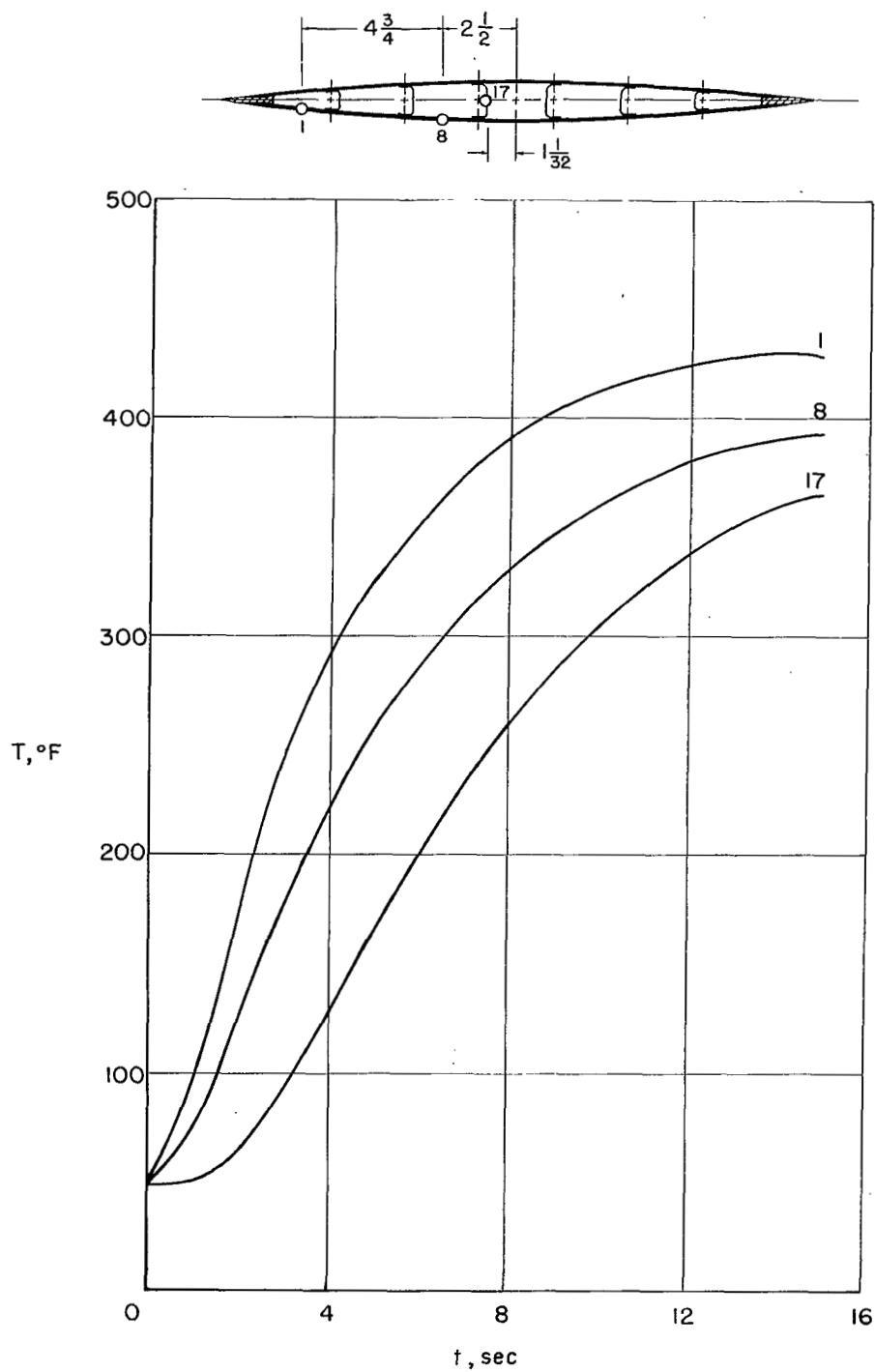
Figure 8.- Typical temperature histories. Model MW-5.
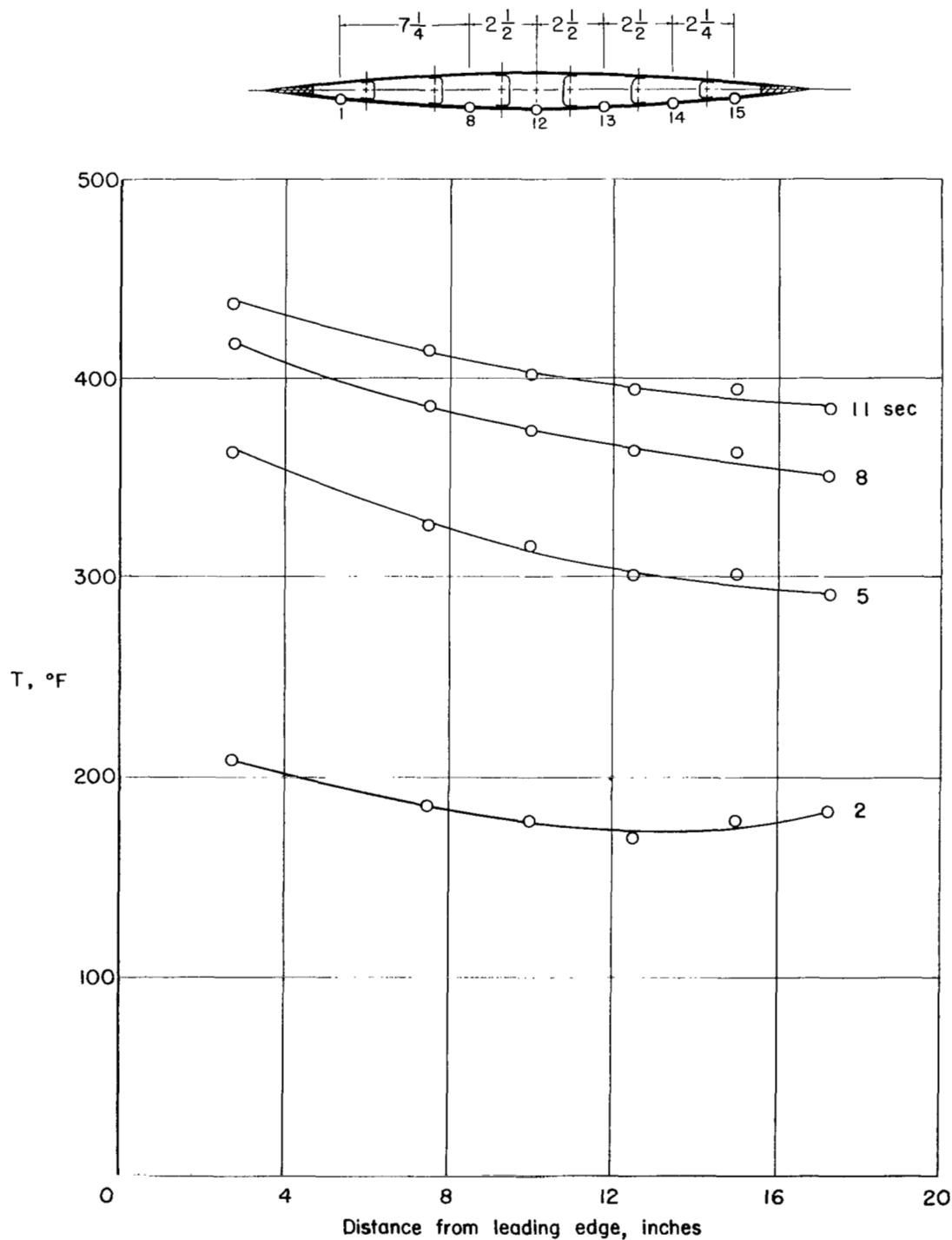
Figure 9.- Chordwise variation of skin temperature.   Model MW-6.
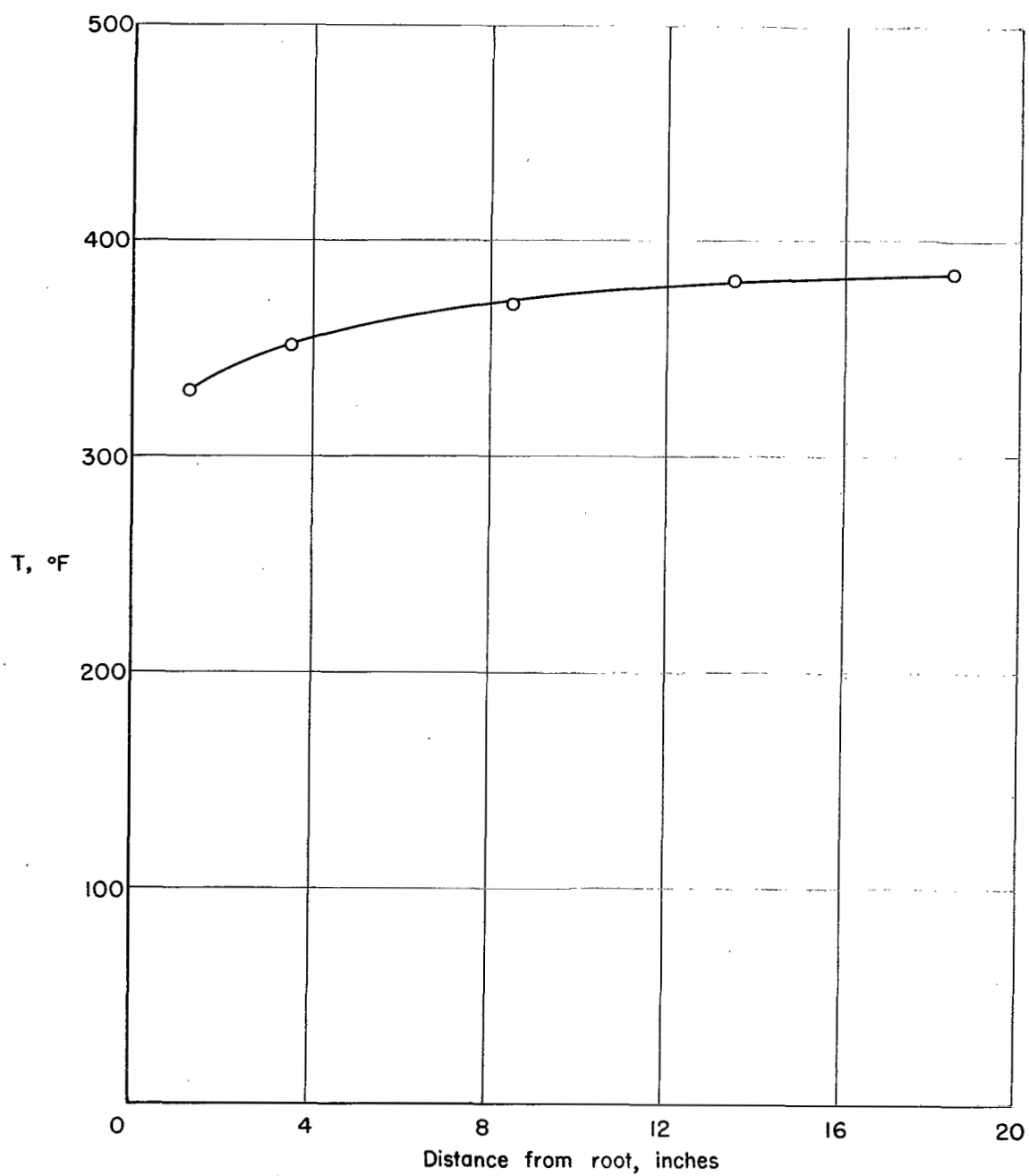
Figure 10.- Spanwise variation of skin temperature. Model MW-7 at
8 seconds.
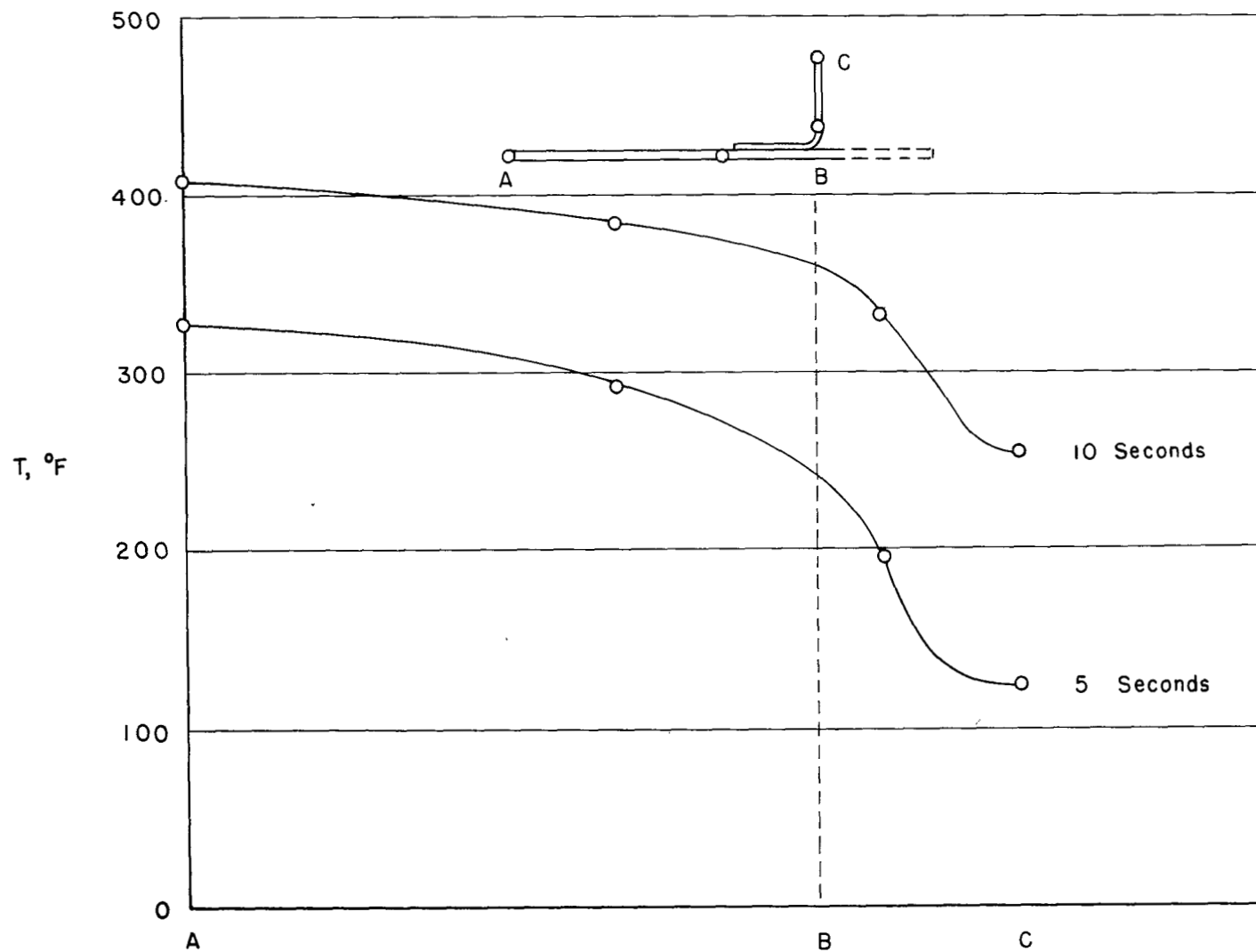
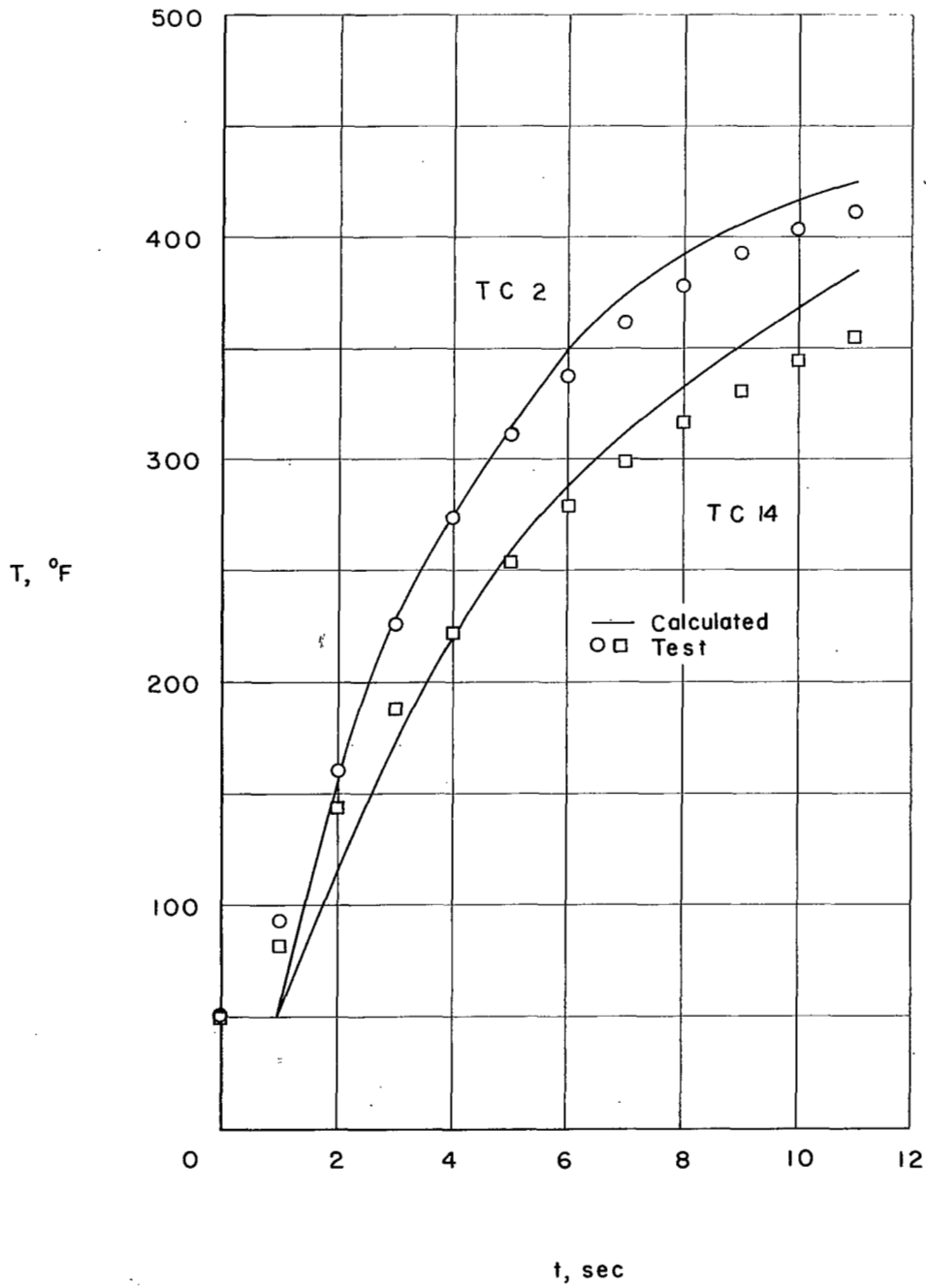Figure 11.- Temperature distribution in skin and web combination. Model MW-6.
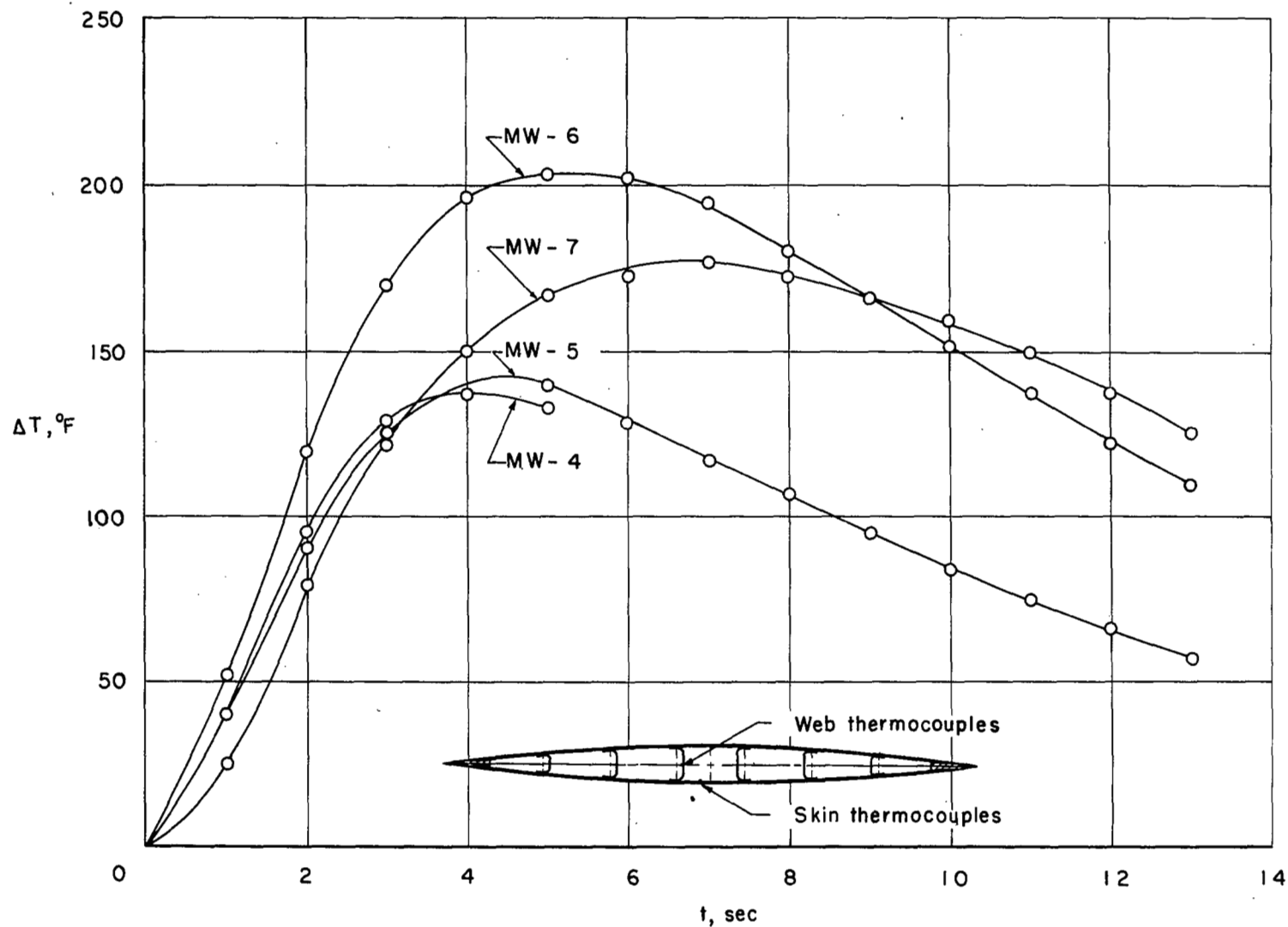
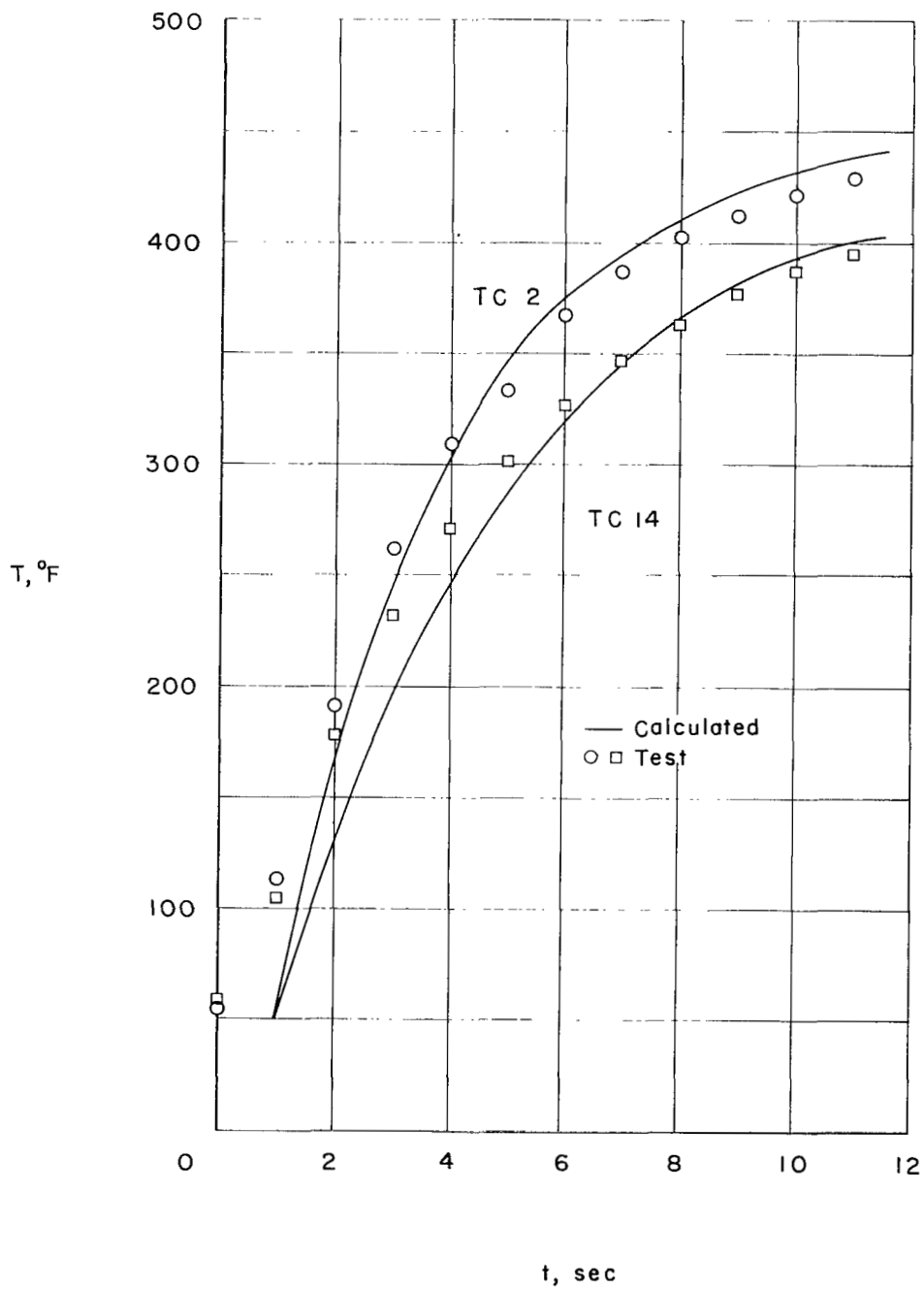Figure 12.- Difference between skin and web temperatures.
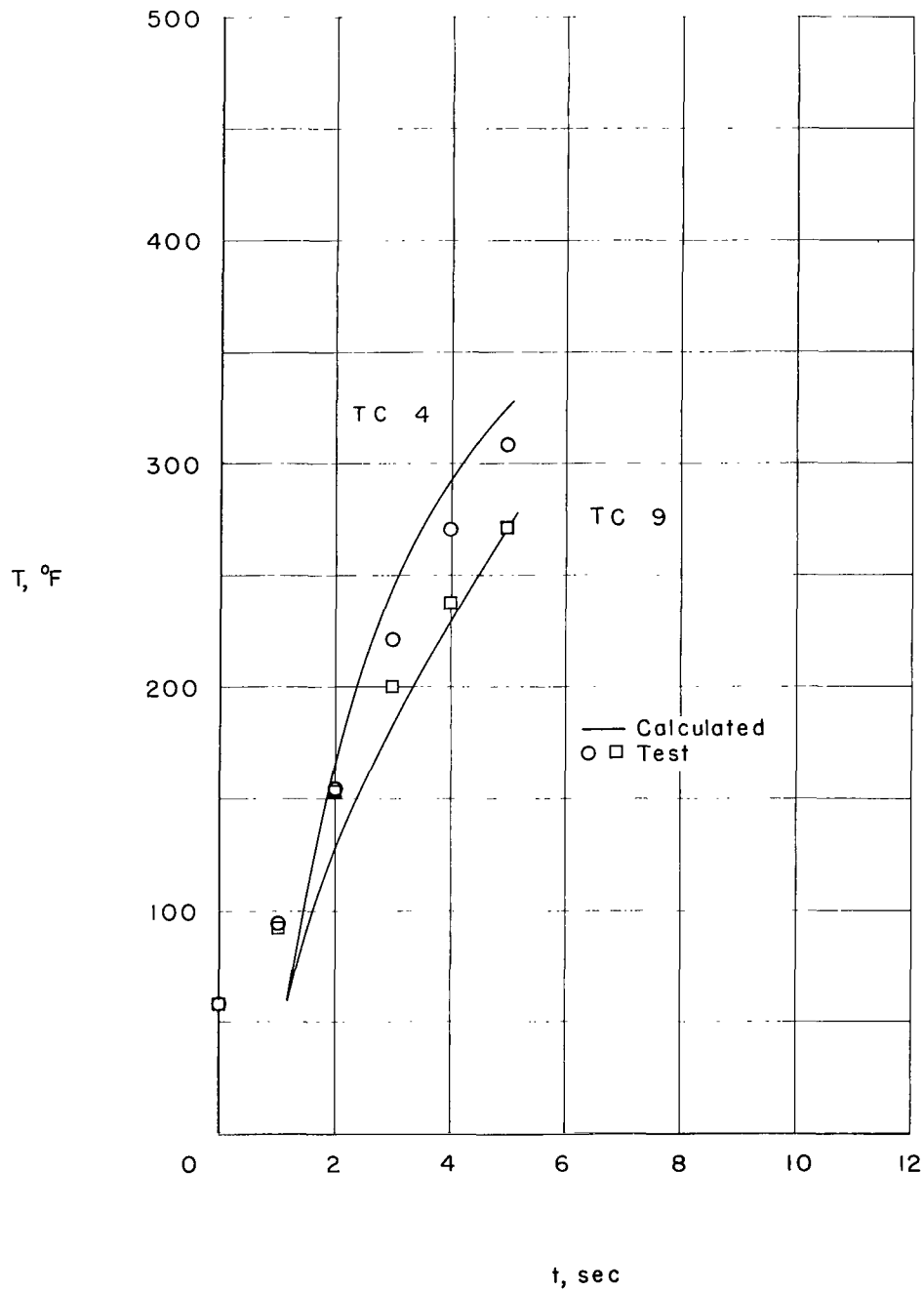
(a) Thermocouples 4 and 9; model MW-4.

Figure 13.- Comparison of calculated and experimental values of skin temperatures.
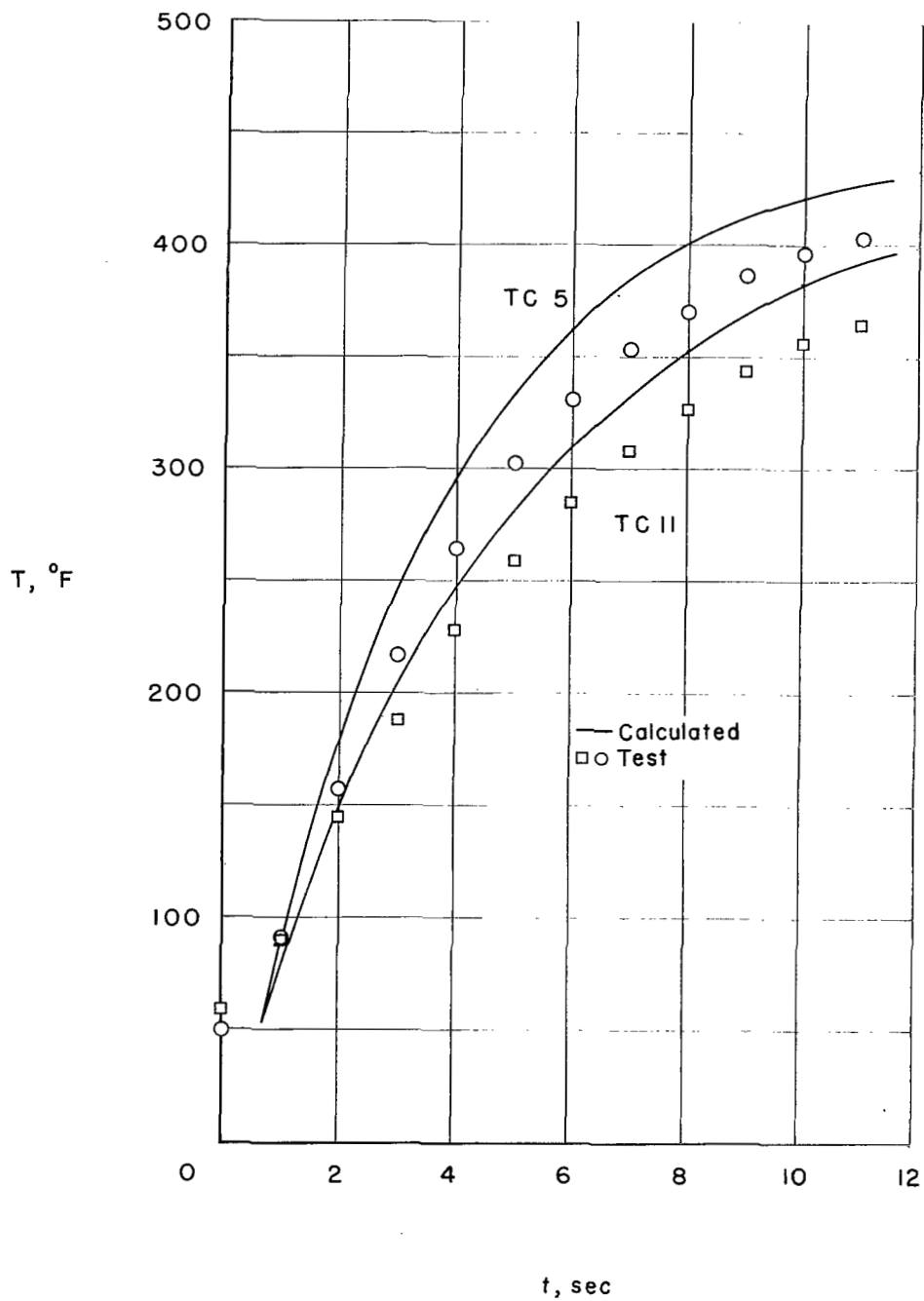
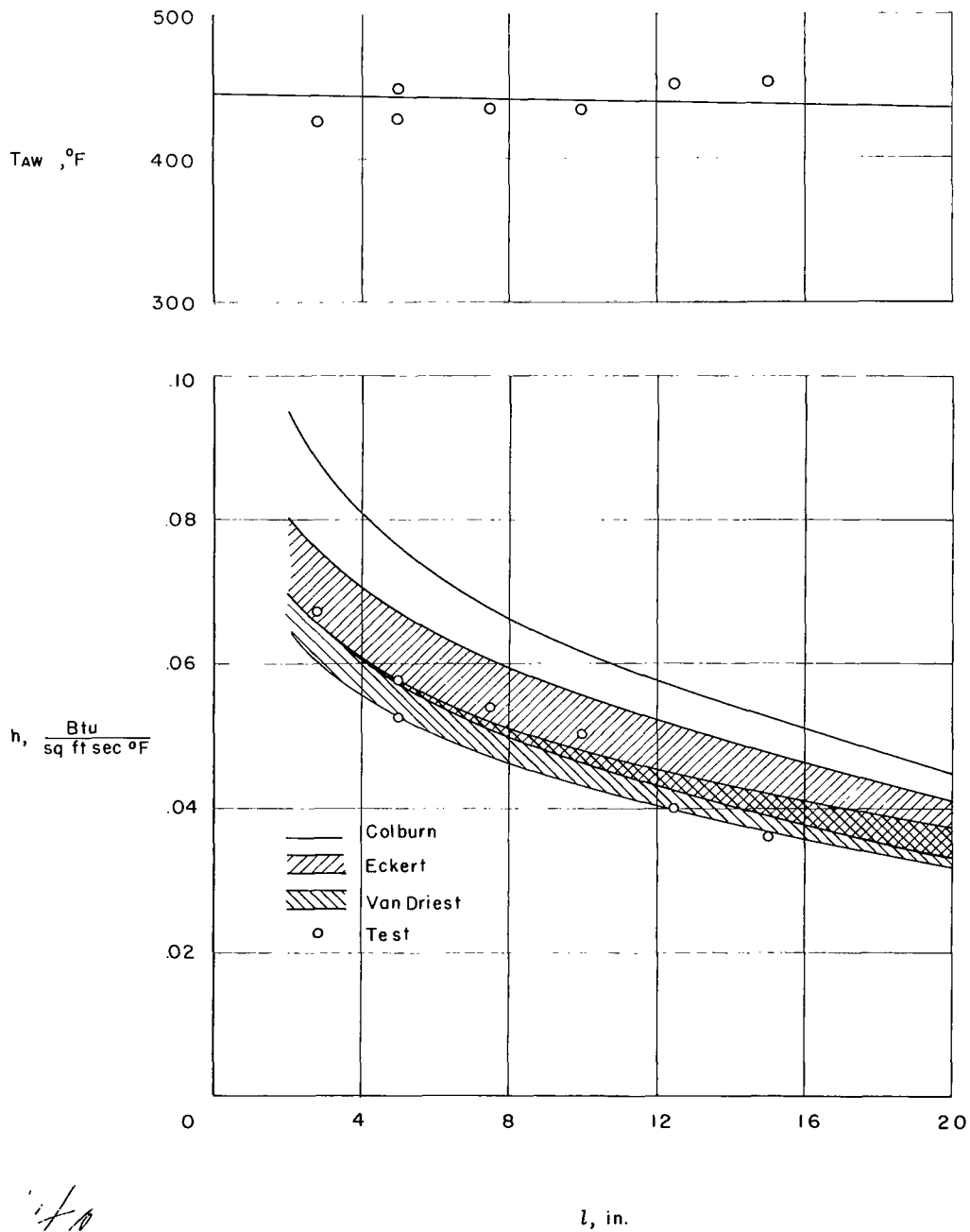(b) Thermocouples 2 and 14; model MW-5.

Figure 13.- Continued.

(c) Thermocouples 2 and 14; model MW-6.
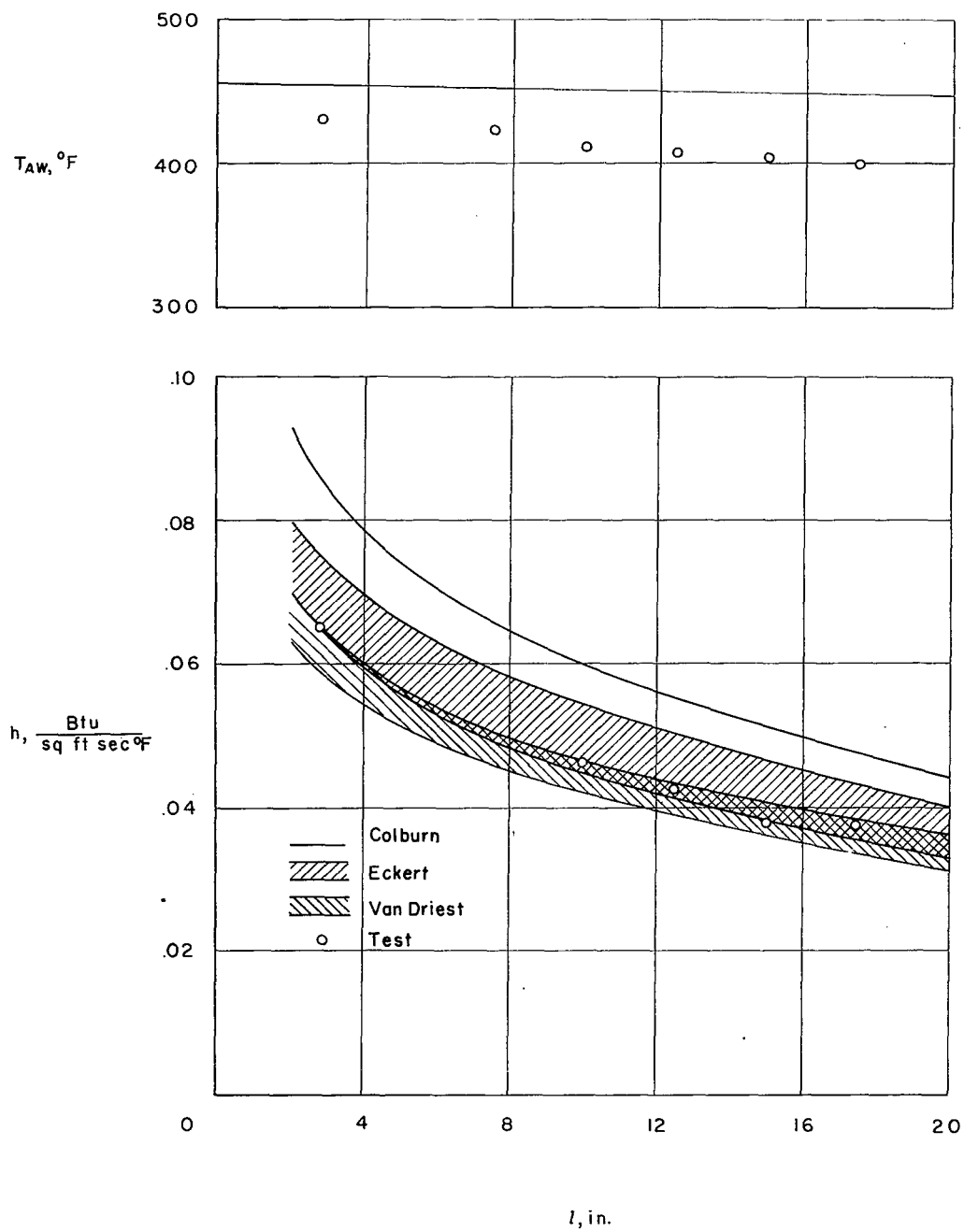
Figure 13.- Continued.

(d) Thermocouples 5 and 11; model MW-7.
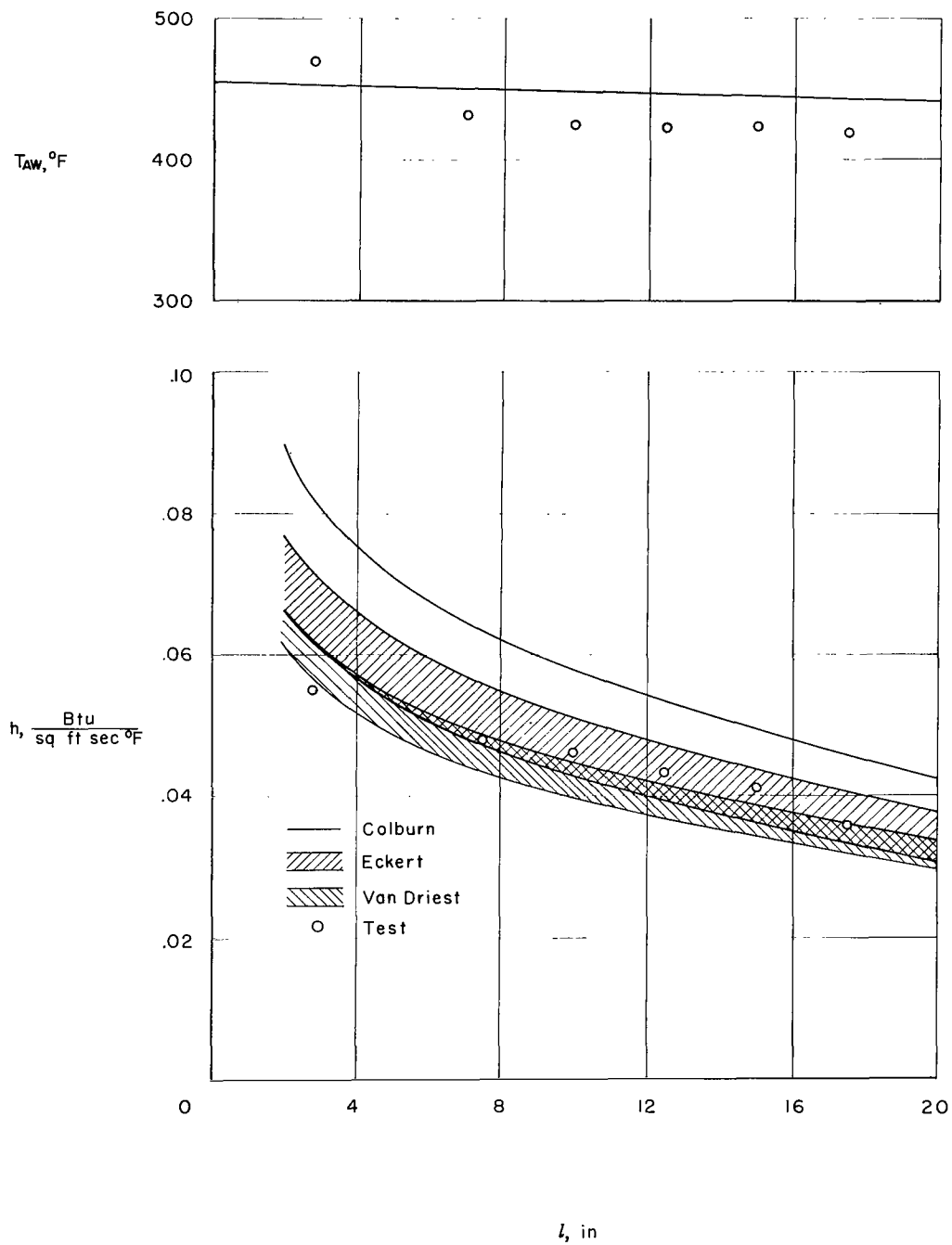
Figure 13.- Concluded.

(a) Model MW-4.

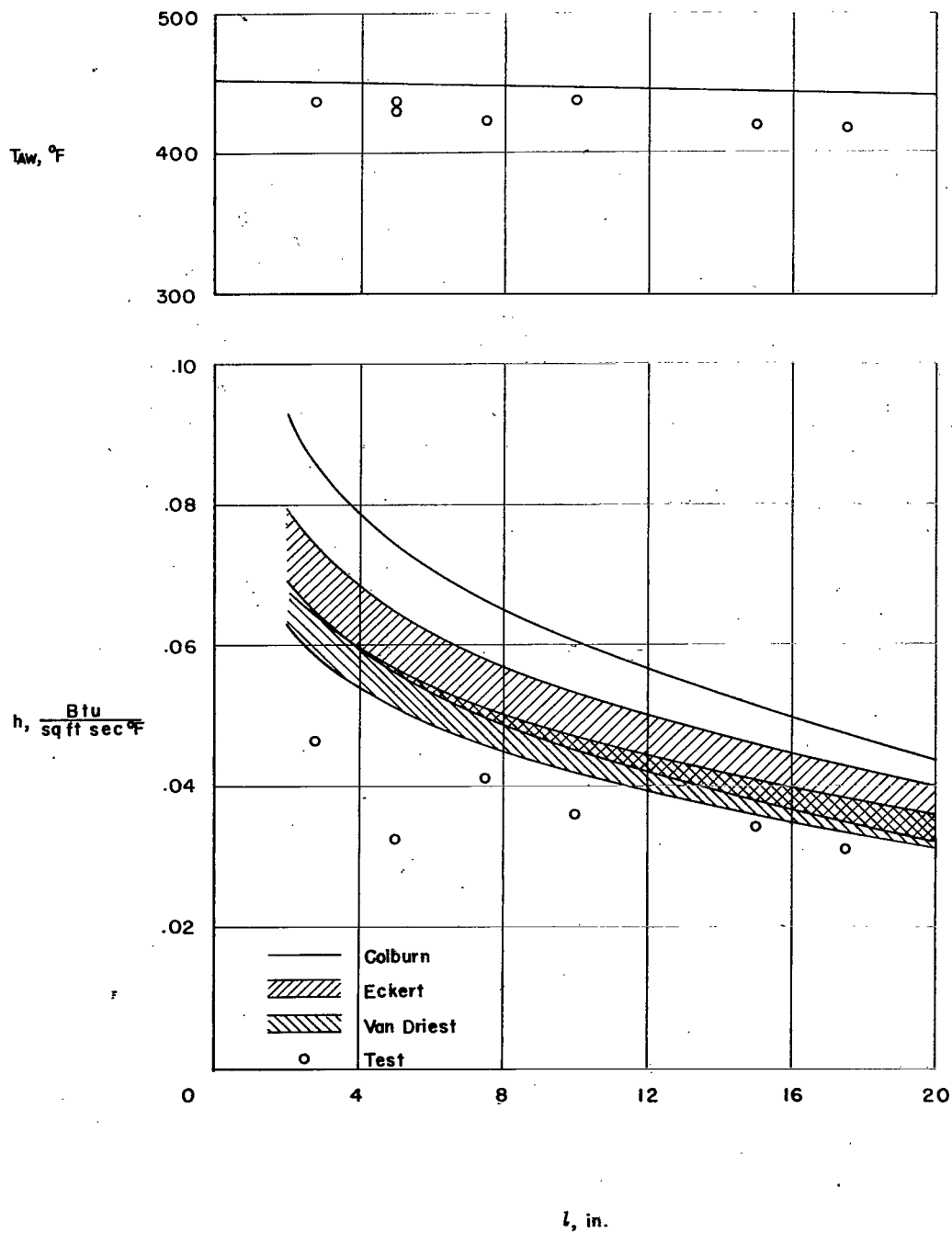Figure 14.- Comparison of calculated and experimental values of T_{aw} and h.

(b) Model MW-5.

Figure 14.- Continued.

(c) Model MW-6.

Figure 14.- Continued.

l, in.

(d) Model MW-7.

Figure 14.- Concluded.

NACA RM L57H01

A motion-picture film supplement, carrying the same classification
as the report, is available on loan. Requests will be filled in the
order received. You will be notified of the approximate date scheduled.

The film $\left(16 \text{ mm.}, 3\frac{1}{2} \text{ min.}, \text{B\&W, silent}\right)$ shows the entire test of
model MW-4 from each side and from overhead with pictures taken at about
128 frames per second. The failure of the model is shown in slower motion
by pictures taken at 625 frames per second.

NOTE: It will expedite the handling of requests for this classified film
if application for the loan is made by the individual to whom this copy
of the report was issued. In line with established policy, classified
material is sent only to previously designated individuals. Your coopera-
tion in this regard will be appreciated.

CUT

Date _____

Please send, on loan, copy of film supplement to RM L57H01

Name of organization _____

Street number _____

City and State _____

Attention:* Mr. _____

Title _____

*To whom copy No. ____ of the RM was issued

```
                                              ┌──────────┐  ¦
                                              │  Place   │  ¦
                                              │  stamp   │  ¦
                                              │  here    │  ¦
                                              └──────────┘  ¦
```

Chief, Division of Research Information
National Advisory Committee for Aeronautics
1512 H Street, N. W.
Washington 25, D. C.